

Figure 5 Effects of the M301K mutation on NRVM action potentials. Typical action potentials were demonstrated in a non-transfected cell (A), in a WT-overexpressed cell (B), and in a heterozygous overexpressed cell (C). Graphs show APD at 90% repolarization from the overshoot (D). In WT-overexpressed NRVMs, the plateau phase of the cardiac AP was markedly abbreviated, resulting in short repolarization. Under the heterozygous overexpressed condition, the results exhibited virtually no plateau phase, and the mean APD₉₀ was significantly shorter in comparison with WT overexpressed alone. * $P < 0.001$.

remains unknown why only tentative hetero-multimers of WT and M301K are active and lose their inward rectification properties. In homozygous M301K channels, all of the tetrameric subunits must have a positively charged lysine at 301, which may impair potassium ion permeation due to a conformational change in the near-pore region.

4.4 Heterozygous *KCNJ2*-WT/M301K overexpression shortened APD in NRVMs

In cardiomyocytes, Kir2.1, Kir2.2, and Kir2.3 channels are supposed to be able to co-assemble in order to modulate their channel properties.²² Thus, there can be a multitude of Kir2.x heteromultimers, and to date a wide range of single-channel conductances of inward rectifier channels have been reported in studies conducted on various mammalian myocytes, including human.^{23–25} This variety at the individual channel level may contribute to the different stoichiometry of the tetrameric channels.²⁶ Because Kir2.1 is a major component of IK1 in the myocardium, we overexpressed the *KCNJ2* M301K mutant channels in NRVMs to examine the effects of the mutation on APD. Overexpression with WT alone resulted in shorter APD in comparison with non-transfected myocytes (Figure 5B). These results are consistent with a previously published report.²⁷ Notably, heterozygous overexpression with WT and M301K further

amplified the shortened APD (Figure 5C). These results were compatible with the electrophysiological changes assessed in HEK 293 cells, because the heterozygous WT/M301K channels showed a larger outward current than WT Kir2.1 channels under the physiological range of membrane potentials (Figure 3). Weak inward rectification observed in the heterozygous WT/M301K channels suggests that potassium ion can get through Kir2.1 channel at depolarized potential, probably resulting in loss of the action potential dome recorded in the *KCNJ2* WT/M301K-overexpressed group. The experiments were performed using a transient overexpression system that was different from the patient's heart, and the amount of overexpressed channels was difficult to be estimated accurately. But, these results are beneficial in understanding that the heterozygous *KCNJ2* M301K mutation could abbreviate APD and cause an extremely short-QT interval in the patient's ECG.

4.5 Clinical features of the index patient with *KCNJ2*-M301K

Regarding the clinical criteria for the diagnosis of SQTs, they have yet to be defined. However, we should consider SQTs in a patient presenting with a QTc < 340 ms and other factors suggestive of arrhythmia (such as syncope or family history of sudden death).²⁸ A prominent clinical manifestation of SQTs is arrhythmias, such as AF

and VF.^{1–5,7} In this patient, however, additional medical histories not limited to arrhythmias, such as severe mental retardation, abnormal proliferation of the oesophageal blood vessels, epilepsy, and Kawasaki disease, were also documented. Because *KCNJ2* is known to be expressed in a variety of tissues, such as cardiac and skeletal muscle, the brain, arterial smooth muscle cells and developing bony structures of the craniofacial region, extremities, and vertebrae,^{29–31} some of her compound disorders may be attributed to the *KCNJ2* mutation. In fact, loss-of-function mutations in *KCNJ2* cause Andersen–Tawil syndrome, which is characterized by prolonged repolarization, dysmorphic features, and periodic paralysis.^{10,32} In the family of our female patient, we could not perform extensive genetic testing. We cannot exclude the possibility of the presence of other affected genes. Further analyses using knock-in mice or induced pluripotent stem cells would culminate monumental insight into the relationship between the *KCNJ2* M301K mutation and the patient's extra-cardiac phenotypes.

4.6 Conclusions

We described a novel *KCNJ2* gain-of-function mutation, M301K, in a patient with SQTs. Functional assays revealed no functional currents in the homozygous channels, whereas impaired inward rectification in the heterozygous channels manifested in larger outward currents, which is a novel mechanism predisposing SQTs.

Acknowledgements

We thank Dr Richard H. Kaszynski at the Kobe University School of Medicine for his critical reading of this manuscript.

Conflict of interest: none declared.

Funding

This work was supported by research grants from the Ministry of Education, Culture, Science, and Technology of Japan (T.M. and M.H.), the Takeda Science Foundation (T.M.), the Miyata Cardiac Research Promotion Foundation (T.M.), Japan Heart Foundation/Novartis Grant for Research Award on Molecular and Cellular Cardiology (T.M.), the Uehara Memorial Foundation (M.H.), Suzuken Memorial Foundation (T.K.), and health science research grants from the Ministry of Health, Labor, and Welfare of Japan for Clinical Research on Measures for Intractable Diseases (T.M. and M.H.).

References

- Gussak I, Brugada P, Brugada J, Wright RS, Kopecky SL, Chaitman BR et al. Idiopathic short QT interval: a new clinical syndrome? *Cardiology* 2000;**94**:99–102.
- Brugada R, Hong K, Dumaine R, Cordeiro J, Gaita F, Borggrefe M et al. Sudden death associated with short-QT syndrome linked to mutations in HERG. *Circulation* 2004;**109**:30–35.
- Bellocq C, van Ginneken AC, Bezzina CR, Alders M, Escande D, Mannens MM et al. Mutation in the *KCNQ1* gene leading to the short QT-interval syndrome. *Circulation* 2004;**109**:2394–2397.
- Priori SG, Pandit SV, Rivolta I, Berenfeld O, Ronchetti E, Dhamoon A et al. A novel form of short QT syndrome (SQT3) is caused by a mutation in the *KCNJ2* gene. *Circ Res* 2005;**96**:800–807.
- Antzelevitch C, Pollevick GD, Cordeiro JM, Casis O, Sanguinetti MC, Aizawa Y et al. Loss-of-function mutations in the cardiac calcium channel underlie a new clinical entity characterized by ST-segment elevation, short QT intervals, and sudden cardiac death. *Circulation* 2007;**115**:442–449.

- Templin C, Ghadri JR, Rougier JS, Baumer A, Kaplan V, Albesa M et al. Identification of a novel loss-of-function calcium channel gene mutation in short QT syndrome (SQTs6). *Eur Heart J* 2011;**32**:1077–1088.
- Hong K, Piper DR, Diaz-Valdecantos A, Brugada J, Oliva A, Burashnikov E et al. De novo *KCNQ1* mutation responsible for atrial fibrillation and short QT syndrome in utero. *Cardiovasc Res* 2005;**68**:433–440.
- Garberoglio L, Giustetto C, Wolpert C, Gaita F. Is acquired short QT due to digitalis intoxication responsible for malignant ventricular arrhythmias? *J Electrocardiol* 2007;**40**:43–46.
- Akao M, Ohler A, O'Rourke B, Marban E. Mitochondrial ATP-sensitive potassium channels inhibit apoptosis induced by oxidative stress in cardiac cells. *Circ Res* 2001;**88**:1267–1275.
- Haruna Y, Kobori A, Makiyama T, Yoshida H, Akao M, Doi T et al. Genotype-phenotype correlations of *KCNJ2* mutations in Japanese patients with Andersen-Tawil syndrome. *Hum Mutat* 2007;**28**:208.
- Ma D, Tang XD, Rogers TB, Welling PA. An Andersen-Tawil syndrome mutation in Kir2.1 (V302M) alters the G-loop cytoplasmic K⁺ conduction pathway. *J Biol Chem* 2007;**282**:5781–5789.
- Ballester LY, Benson DW, Wong B, Law IH, Mathews KD, Vanoye CG et al. Trafficking-competent and trafficking-defective *KCNJ2* mutations in Andersen syndrome. *Hum Mutat* 2006;**27**:388.
- Pegan S, Arrabit C, Zhou W, Kwiatkowski W, Collins A, Slesinger PA et al. Cytoplasmic domain structures of Kir2.1 and Kir3.1 show sites for modulating gating and rectification. *Nat Neurosci* 2005;**8**:279–287.
- Tai K, Stansfeld PJ, Sansom MS. Ion-blocking sites of the Kir2.1 channel revealed by multiscale modeling. *Biochemistry* 2009;**48**:8758–8763.
- Fujiwara Y, Kubo Y. Functional roles of charged amino acid residues on the wall of the cytoplasmic pore of Kir2.1. *J Gen Physiol* 2006;**127**:401–419.
- Gollob MH, Redpath CJ, Roberts JD. The short QT syndrome: proposed diagnostic criteria. *J Am Coll Cardiol* 2011;**57**:802–812.
- Xia M, Jin Q, Bendahhou S, He Y, Larroque MM, Chen Y et al. A Kir2.1 gain-of-function mutation underlies familial atrial fibrillation. *Biochem Biophys Res Commun* 2005;**332**:1012–1019.
- Matsuda H, Saigusa A, Irisawa H. Ohmic conductance through the inwardly rectifying K channel and blocking by internal Mg²⁺. *Nature* 1987;**325**:156–159.
- Horie M, Irisawa H, Noma A. Voltage-dependent magnesium block of adenosine-triphosphate-sensitive potassium channel in guinea-pig ventricular cells. *J Physiol* 1987;**387**:251–272.
- Hille B. *Ion Channels of Excitable Membranes*. Sunderland: Sinauer Associates, 2001.
- Robertson JL, Palmer LG, Roux B. Long-pore electrostatics in inward-rectifier potassium channels. *J Gen Physiol* 2008;**132**:613–632.
- Liu Y, Fowler CD, Wang Z. Ontogeny of brain-derived neurotrophic factor gene expression in the forebrain of prairie and montane voles. *Brain Res Dev Brain Res* 2001;**127**:51–61.
- Nakamura TY, Artman M, Rudy B, Coetzee WA. Inhibition of rat ventricular IK1 with antisense oligonucleotides targeted to Kir2.1 mRNA. *Am J Physiol* 1998;**274**:H892–H900.
- Picones A, Keung E, Timpe LC. Unitary conductance variation in Kir2.1 and in cardiac inward rectifier potassium channels. *Biophys J* 2001;**81**:2035–2049.
- Wible BA, De Biasi M, Majumder K, Tagliatela M, Brown AM. Cloning and functional expression of an inwardly rectifying K⁺ channel from human atrium. *Circ Res* 1995;**76**:343–350.
- Preisig-Muller R, Schlichthorl G, Goerge T, Heinen S, Bruggemann A, Rajan S et al. Heteromerization of Kir2.x potassium channels contributes to the phenotype of Andersen's syndrome. *Proc Natl Acad Sci USA* 2002;**99**:7774–7779.
- Miake J, Marban E, Nuss HB. Functional role of inward rectifier current in heart probed by Kir2.1 overexpression and dominant-negative suppression. *J Clin Invest* 2003;**111**:1529–1536.
- Viswanathan MN, Page RL. Short QT: when does it matter? *Circulation* 2007;**116**:686–688.
- Raab-Graham KF, Radeke CM, Vandenberg CA. Molecular cloning and expression of a human heart inward rectifier potassium channel. *Neuroreport* 1994;**5**:2501–2505.
- Karkanis T, Li S, Pickering JG, Sims SM. Plasticity of KIR channels in human smooth muscle cells from internal thoracic artery. *Am J Physiol Heart Circ Physiol* 2003;**284**:H2325–H2334.
- Karschin C, Karschin A. Ontogeny of gene expression of Kir channel subunits in the rat. *Mol Cell Neurosci* 1997;**10**:131–148.
- Plaster NM, Tawil R, Tristani-Firouzi M, Canun S, Bendahhou S, Tsunoda A et al. Mutations in Kir2.1 cause the developmental and episodic electrical phenotypes of Andersen's syndrome. *Cell* 2001;**105**:511–519.

Regional cooling facilitates termination of spiral-wave reentry through unpinning of rotors in rabbit hearts

Masatoshi Yamazaki, MD, PhD,^{*†} Haruo Honjo, MD, PhD,^{*†} Takashi Ashihara, MD, PhD,[‡] Masahide Harada, MD, PhD,^{*} Ichiro Sakuma, PhD,[§] Kazuo Nakazawa, PhD,^{||} Natalia Trayanova, PhD, FHRS, FAHA,[¶] Minoru Horie, MD, PhD,[‡] Jérôme Kalifa, MD, PhD,[†] José Jalife, MD, FHRS,[†] Kaichiro Kamiya, MD, PhD,^{*} Itsuo Kodama, MD, PhD^{*}

From the ^{*}Department of Cardiovascular Research, Research Institute of Environmental Medicine, Nagoya University, Nagoya, Japan, [†]Center for Arrhythmia Research, University of Michigan, Ann Arbor, Michigan, [‡]Department of Cardiovascular and Respiratory Medicine, Shiga University of Medical Science, Otsu, Japan, [§]Graduate School of Engineering, The University of Tokyo, Tokyo, Japan, ^{||}National Cardiovascular Center, Research Institute, Suita, Japan, [¶]Institute for Computational Medicine, Johns Hopkins University, Baltimore, Maryland.

BACKGROUND Moderate global cooling of myocardial tissue was shown to destabilize 2-dimensional (2-D) reentry and facilitate its termination.

OBJECTIVE This study sought to test the hypothesis that regional cooling destabilizes rotors and facilitates termination of spontaneous and DC shock-induced subepicardial reentry in isolated, endocardially ablated rabbit hearts.

METHODS Fluorescent action potential signals were recorded from 2-D subepicardial ventricular myocardium of Langendorff-perfused rabbit hearts. Regional cooling (by $5.9^{\circ}\text{C} \pm 1.3^{\circ}\text{C}$) was applied to the left ventricular anterior wall using a transparent cooling device (10 mm in diameter).

RESULTS Regional cooling during constant stimulation (2.5 Hz) prolonged the action potential duration (by $36\% \pm 9\%$) and slightly reduced conduction velocity (by $4\% \pm 4\%$) in the cooled region. Ventricular tachycardias (VTs) induced during regional cooling terminated earlier than those without cooling (control): VTs lasting >30 seconds were reduced from 17 of 39 to 1 of 61. When regional cooling was applied during sustained VTs (>120 seconds), 16 of 33 (48%) sustained VTs self-terminated in 12.5 ± 5.1 seconds. VT termination was the result of rotor destabilization,

which was characterized by unpinning, drift toward the periphery of the cooled region, and subsequent collision with boundaries. The DC shock intensity required for cardioversion of the sustained VTs decreased significantly by regional cooling (22.8 ± 4.1 V, $n = 16$, vs 40.5 ± 17.6 V, $n = 21$). The major mode of reentry termination by DC shocks was phase resetting in the absence of cooling, whereas it was unpinning in the presence of cooling.

CONCLUSION Regional cooling facilitates termination of 2-D reentry through unpinning of rotors.

KEYWORDS Spiral-wave reentry; Regional myocardial cooling; Unpinning; Optical mapping; Ventricular tachyarrhythmia

ABBREVIATIONS 2-D = two-dimension; 3-D = three-dimension; APD = action potential duration; BCL = basic cycle length; BDM = 2,3-butandione monoxime; CV = conduction velocity; FBL = functional block line; ICD = implantable cardioverter-defibrillator; LV = left ventricle; PS = phase singularity; RC = regional cooling; SW = spiral wave; VF = ventricular fibrillation; VT = ventricular tachycardia

(Heart Rhythm 2012;9:107–114) © 2012 Heart Rhythm Society. All rights reserved.

Introduction

High-energy DC shock application by implantable cardioverter-defibrillator (ICD) is the most effective procedure for preventing sudden cardiac death resulting from ventricular tachycardia/ventricular fibrillation (VT/VF). Large-scale

clinical trials have demonstrated that ICD therapy is superior over any pharmacological therapy to prevent cardiac death.^{1,2} The usefulness of ICD therapy currently available is, however, limited by a number of adverse effects of high-energy shocks, such as myocardial damages causing arrhythmias, increased pacing threshold,^{3,4} and mechanical dysfunction giving rise to hemodynamic deterioration.⁵ In addition, painful DC shocks by ICD often cause serious psychological disorders.^{6,7} Theoretical and experimental studies have revealed that spiral-wave (SW) reentry rotating around a functional obstacle is the major mechanism of VT/VF.^{8,9} Arguably, should SW reentry be regulatable by procedures other than DC shocks or those combined with low-energy shocks, it could lead to innovative therapeutic

This study was supported by Grant-in-Aid for Scientific Research (B) 19390210 and (C) 20590860 from the Japanese Society for Promotion of Sciences and Grant-in-Aid for Scientific Research on Innovative Area 22136010 from the Ministry of Education, Culture, Sports, Science and Technology, Japan. **Address reprint requests and correspondence:** Dr. Haruo Honjo, Department of Cardiovascular Research, Research Institute of Environmental Medicine, Nagoya University, Furo-cho, Chikusa-ku, Nagoya 464-8601, Japan. E-mail address: honjo@riem.nagoya-u.ac.jp.

modalities for prevention of arrhythmic death. Although several conceptual approaches have been proposed to terminate SW reentry by low-energy DC application, e.g., resonant drift,^{10,11} controlling chaos,¹² synchronized pacing,^{13,14} and unpinning of SWs,^{15,16} feasibility of these approaches has not yet been validated. In isolated rabbit hearts, we have previously shown that moderate hypothermia facilitates termination of VT through destabilization (unpinning) of SW reentry.¹⁷ Using high-density electrode mapping in rabbit hearts, Boersma et al¹⁸ demonstrated that regional cooling (RC) of the ventricle during programmed electrical stimulation prevented stabilization of functional reentry and resulted in only brief episodes of polymorphic VT that terminated spontaneously. Here we hypothesized that moderate RC of the ventricular myocardium could be a novel procedure to destabilize already-established and sustained VT and lead to its termination. To test this hypothesis, we carried out high-resolution optical mapping experiments in 2-dimensional (2-D) ventricular myocardium.

Methods

Experimental model and optical mapping

The protocol was approved by the Institutional Animal Care and Use Committee at Nagoya University. The experimental model and procedures of optical mapping are essentially the same as reported previously.^{17,19,20} Briefly, optical membrane potential signals were recorded from a 2-D ventricular muscle layer of Langendorff-perfused rabbit hearts subjected to endocardial cryoablation; 2,3-butandione mon-

oxime (BDM) was applied to minimize motion artifacts. Action potential duration (APD) and conduction velocity (CV) were measured during constant pacing (basic cycle length [BCL] 180 to 400 ms) from the apex. The details of experimental procedures and data analysis are described in the Online Supplemental Methods.

RC

The temperature of the central region of the left ventricular (LV) free wall was temporarily reduced by applying a transparent cooling device (diameter, 10 mm) perfused with cold water and in abutting contact with the epicardial surface (Figure 1A). In pilot experiments using thermography (TVS-200, Nippon Avionics, Tokyo, Japan) (Figure 1B), we confirmed that the temperature in the target area was decreased by $5.9^{\circ}\text{C} \pm 1.3^{\circ}\text{C}$ ($n = 7$, $P < .05$) from baseline (36.0°C). The temperature change was reversed completely after removal of the device. Temperature outside the cooled region remained unchanged.

Experimental protocols

Reentrant VTs (lasting ≥ 3 beats) were induced by modified cross-field stimulation using 1 of 2 protocols. First, in 8 hearts, VTs were induced before and 20 seconds after application of RC to compare their duration and dynamics. Second, in 15 additional hearts, sustained VTs (>120 seconds) were induced and RC was applied to observe its effects on VT duration and dynamics. If the sustained VTs did not terminate during the 30-second observation period of RC, 10-ms monophasic DC shocks were applied at in-

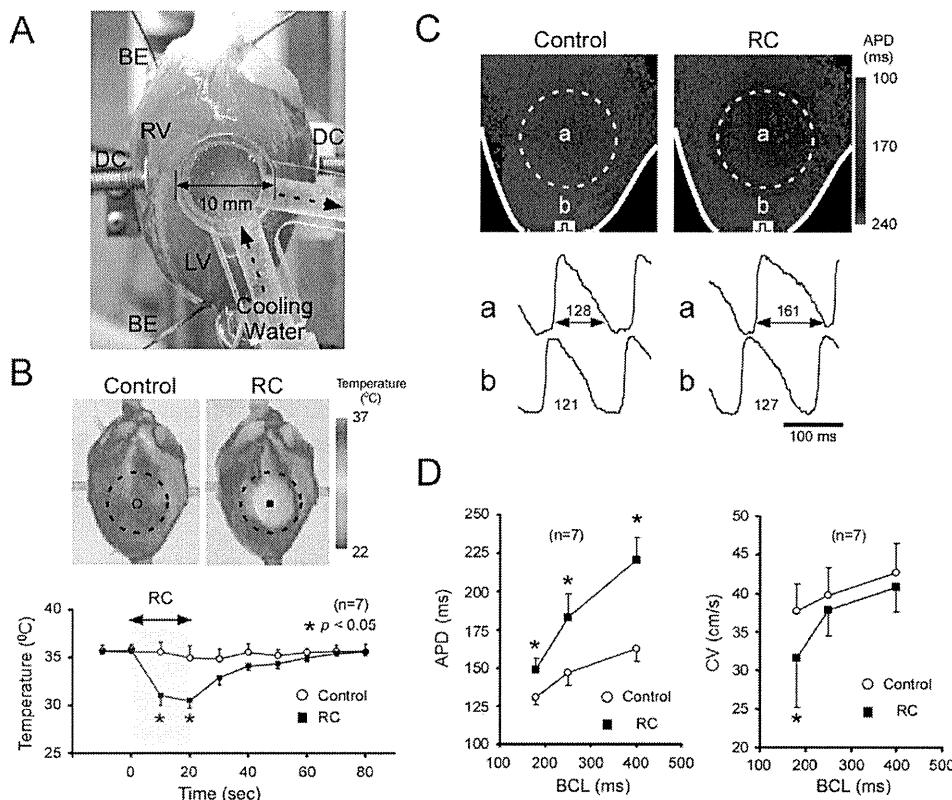


Figure 1 RC of 2-D rabbit hearts. **A:** A transparent cooling device (diameter, 10 mm) was in contact with the LV subepicardial surface, and water (20°C) was circulated inside the device. **B:** Thermography images (top) and changes of temperature (bottom) in response to RC. Those without RC served as control. $*P < .05$ vs control. **C:** Changes of APD (BCL, 400 ms) in response to RC. Top, APD color gradient maps with and without RC (control); bottom, optical action potential signals inside (a) and outside (b) the RC region. Numerals are APD (in ms). **D:** Effects of RC on APD (left) and CV (right) in the RC region at BCLs 180 to 400 ms. $*P < .05$ vs control (without RC). 2-D = two-dimensional; APD = action potential duration; BCL = basic cycle length; BE = electrodes for recording distant bipolar electrograms; CV = conduction velocity; DC = paddle electrodes for DC-application; LV = left ventricle; RC = regional cooling.

creasing or decreasing voltage (by 5 to 10 V in steps from 25 V) to determine the threshold intensity for cardioversion. Sustained VTs without RC served as control subjects.

In 6 rabbits, effects of RC on VT/VF were examined in 3-dimensional (3-D) ventricles without cryoablation. Sustained VT/VFs (>120 seconds) were induced, and cardioversion by RC alone or in combination with DC shocks (8/2-ms biphasic, 25 to 100 V) was attempted.

Statistical analysis

Data are expressed as mean \pm SD. Statistical comparisons were performed by 2-way analysis of variance with Bonferroni post hoc test or Welch 2-sample *t* test when appropriate. Differences were considered significant when $P < .05$.

Results

APD and CV during constant pacing

Effects of RC on APD and CV were examined in 7 hearts. Representative changes in APD (BCL, 400 ms) are shown in Figure 1C. Cooling (20 seconds) increased APD in the RC region, whereas APD outside the RC region was unchanged. Figure 1D summarizes the changes of APD and CV in the RC region. RC caused a significant increase of APD (BCLs, 180 to 400 ms); the longer the BCL, the greater the APD prolongation. RC decreased CV, although the changes remained statistically insignificant at BCLs 250 and 400 ms.

In 3 hearts, all of the RC-induced changes of APD and CV were reversed completely within 60 seconds after removal of the cooling device (data not shown).

VT induced during RC application

In 8 hearts, VTs were induced before (control) and 20 seconds after RC. In control subjects, 18 of 39 VTs (46%) terminated within 5 seconds, 4 VTs (10%) terminated in 5 to 30 seconds, and 17 VTs (44%) persisted for >30 seconds. During RC, in contrast, 58 of 61 VTs (95%) terminated within 5 seconds, 2 VTs (3%) terminated in 5 to 30 seconds, and 1 VT (2%) persisted >30 seconds. Thus, most of VTs induced during RC terminated earlier than in control subjects. The VT cycle length during RC (178 ± 20 ms, $n = 61$) was significantly longer compared with control subjects (143 ± 23 ms, $n = 39$, $P < .05$). Reversibility of the RC effects on the VT persistence was tested in 3 hearts. The incidence of persisted (>30 seconds)/all VTs was 11 of 23 (48%) in control subjects, 1 of 26 (4%) during RC, and 8 of 13 (62%) 5 to 20 minutes after removal of the cooling device.

Optical images of excitation were analyzed in 5 hearts (9 VTs before RC and 13 VTs during RC) exhibiting visible rotor(s). In control, the rotors were, in most cases (7 of 9) stable with small meandering. The 13 VTs induced during RC, in contrast, were all unstable with remarkable meandering of rotors along the periphery of the RC region, and they terminated shortly. Action potential traces revealed frequent intermittent conduction block in the RC region

with longer APD, giving rise to drift of the reentry circuit (Online Supplementary Figure 1). The rotors terminated by collision with anatomical boundaries in 7 VTs (Online Supplementary Figure 1), whereas by mutual annihilation in the RC region in 2 cases (Online Supplementary Figure 2). The mode of rotor termination was unable to be analyzed in the remaining 4 cases.

Termination of sustained VT by RC

We next examined the effects of RC applied during sustained VTs (lasting >120 seconds). We induced 76 sustained VTs in 15 hearts and observed them for 30 seconds with and without RC (33 VTs with RC, and 43 VTs without RC as control subjects). None of the 43 sustained VTs terminated in control subjects, whereas 16 of 33 (48%) sustained VTs terminated during the observation period with RC. Average time to termination was 12.5 ± 5.1 seconds ($n = 16$).

Optical images of excitation were analyzed in 16 sustained VTs that terminated during the RC application in 8 hearts. Figure 2 shows a representative experiment. Before the RC application, a stable clockwise rotor circulated around a functional block line (FBL) (approximately 5.1 mm); the bipolar electrogram showed a monomorphic pattern (Figure 2A, and Online Supplementary Video 1). A 3-D plot of the phase singularity (PS) trajectory obtained after phase mapping confirmed the stationarity of the rotor activity. Application of RC resulted in a dramatic change of the rotor dynamics and the VT terminated after approximately 10 seconds. Figure 2B shows isochrone maps during the last 3 beats prior to VT termination. A clockwise rotor circulated around a very long and curved FBL in the RC region in beat 1 and 2. The FBL configuration changed beat to beat in such a way that during beat 3 the FBL extended from the RC region to the atrioventricular groove, resulting in termination of reentry. The bipolar electrogram showed a polymorphic pattern before termination. Action potentials (Figure 2C) from the RC region (d) were longer compared with those outside (a–c, e, f), and this provided a substrate for conduction block. In Figure 2D, phase maps (left) and a 3-D plot of the PS trajectory (right) demonstrated that a single PS moved along the periphery of the RC region and collided with the atrioventricular groove (Online Supplementary Video 2). The mode of rotor termination by RC could be analyzed in 6 sustained VTs. In 4 sustained VTs, rotor terminated by drift and subsequent collision of PSs with boundaries, whereas in the remaining 2 cases, by mutual annihilation of PSs with opposite chiralities in the RC region.

RC failed to terminate 17 of 33 (52%) of the sustained VTs. The failure was attributable in part to the topological relationship between the rotor and the RC region. In other words, the success rate of RC cardioversion was relatively high (12 of 19) when the rotation center was located within or in the vicinity of the RC region. However, success was low (4 of 14) when the rotation center was far from the RC region.

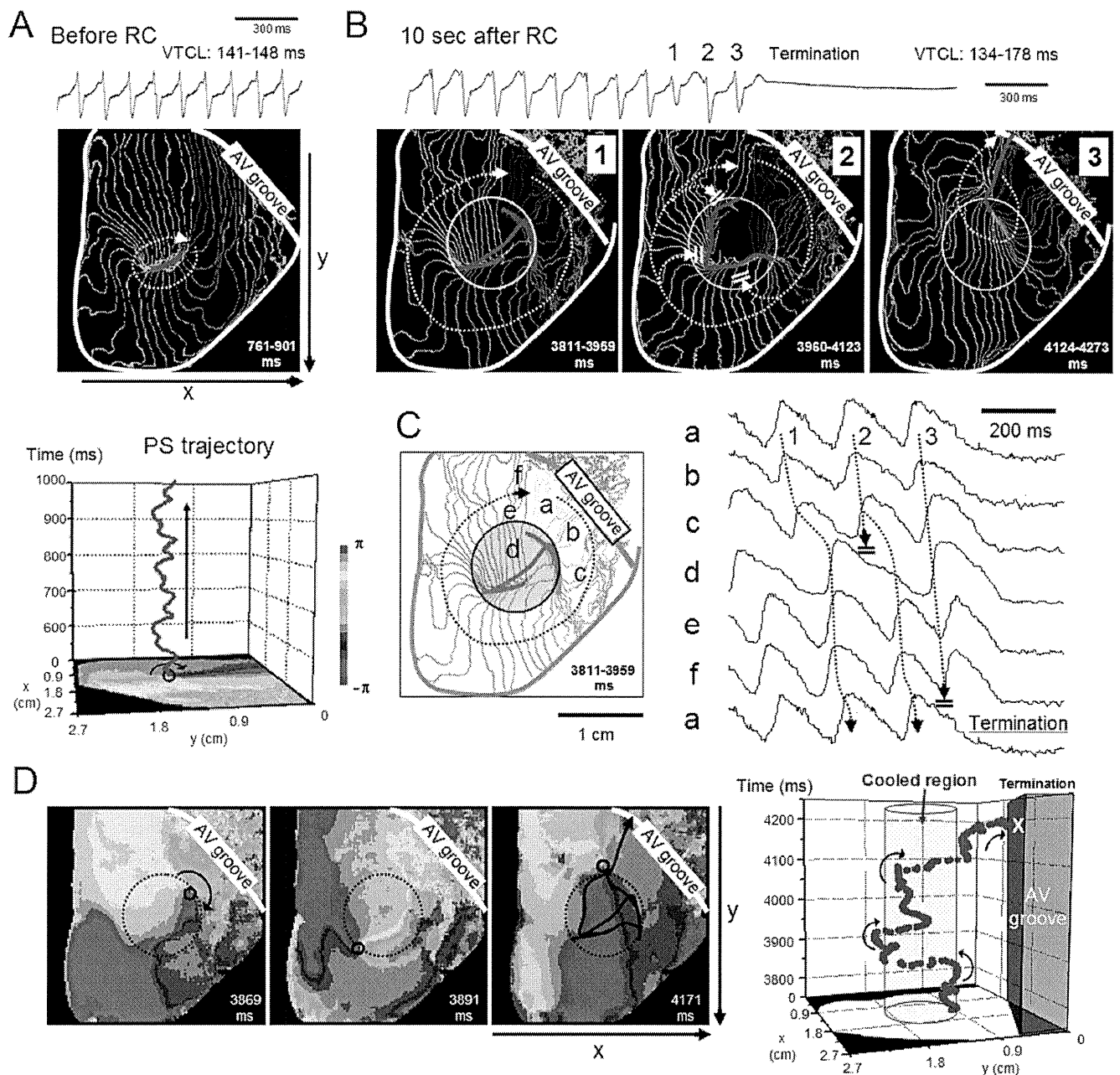


Figure 2 Termination of sustained VT by RC. **A:** Bipolar electrogram (top) and 4-ms isochrone map (middle) of sustained VT (>120 seconds) before RC application. Bottom, trajectory of a PS plotted on space-time axes. Stable reentrant activity was maintained. **B:** Bipolar electrogram (top) and isochrone maps (bottom) of 3 consecutive beats prior to VT termination approximately 10 seconds after RC. A clockwise rotor rotating around a long and curved FBL (pink) changed circuits in each excitation. Yellow circle, RC region. **C:** Optical action potential signals (a-f in the isochrone map) prior to VT termination. Wave propagation was frequently blocked at the periphery of the RC region. **D:** Left, phase maps of the last 2 beats. Black circle, PS of clockwise rotation; dotted circle, RC region. Right, PS trajectory plotted on space-time axes. Blue column, RC region. PS = phase singularity; VT = ventricular tachycardia; other abbreviations as in Figure 1.

Cardioversion of sustained VT by DC shock

When the sustained VTs did not terminate during the 30-second observation period, DC cardioversion was attempted. DC shocks of 15 to 80 V were applied to 21 sustained VTs in the absence of RC (in 12 hearts) and 16 sustained VTs in presence of RC (in 9 hearts) to evaluate the threshold DC shock intensity for cardioversion. The threshold DC shock intensity required for VT termination was

significantly less with RC (22.8 ± 4.1 V, $n = 16$) than that without RC (40.5 ± 17.6 V, $n = 21$, $P < .05$).

The mode of rotor modification and termination by DC shocks with and without RC was also different. Representative experiments are shown in Figure 3. Figure 3A is the consequence of a 25-V shock that failed to terminate the reentrant activity in the absence of RC. A single clockwise rotor (PS1) was present before the DC shock; shock appli-

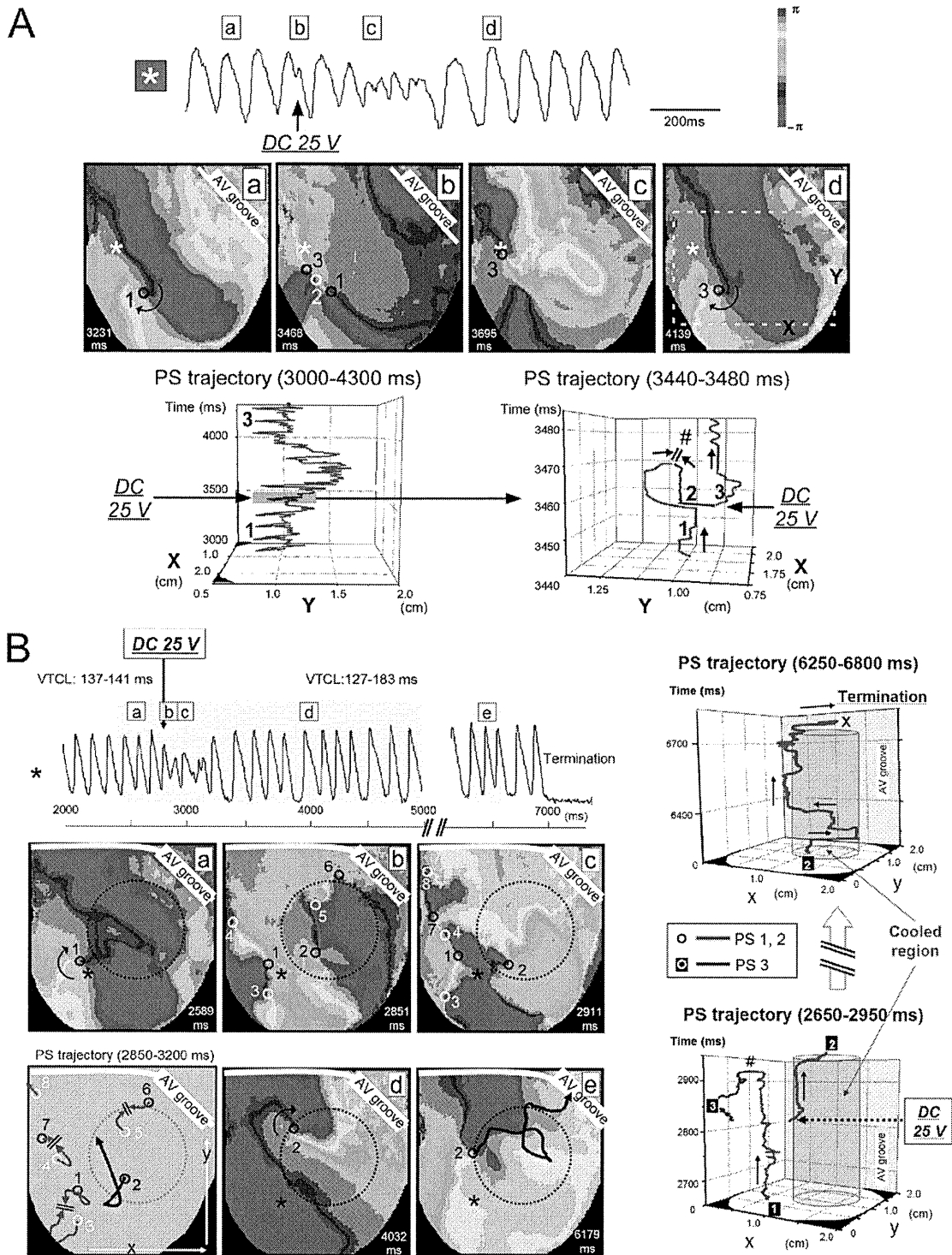


Figure 3 Rotor modification by DC shock applied to sustained VT in the absence and presence of RC. **A:** Failure of cardioversion by low-intensity shock in the absence of RC through repining of PS. Top, action potential trace; middle, phase maps before and after 25-V DC shock application. Black and white circles, PSs of clockwise and counterclockwise rotation, respectively. *Site of action potential recording. Bottom, trajectory of PSs plotted on space-time axes. A part of the trajectory in the left panel (immediately before and after DC shock application) is expanded in the right panel to show generation, mutual annihilation (#), and repining of PSs. **B:** Success of cardioversion by low-intensity DC shock in the presence of RC through unpinning of PS. Left, action potential trace (top) and phase maps (bottom) before (a) and after application of a 25-V DC shock (b–e). The shock application generated new PSs (black and white circles, clockwise and counterclockwise rotation, respectively). Trajectory of the PSs is illustrated in the right bottom panel. PS8 was pushed out of the observation area after meandering. PS1-PS3, PS4-PS7, and PS5-PS6 dissipated by mutual annihilation within 100 ms. PS2 survived and drifted in the periphery of the RC region (unpinning), and collided with the atrioventricular groove. *Site of action potential recording. Right, trajectory of PSs 1-3 plotted on space-time axes. Blue columns indicate the RC region. Abbreviations as in Figure 2.

cation generated a pair of PSs (counterclockwise PS2 and clockwise PS3). Then, PS1 and PS2 collided with each other and disappeared, whereas PS3 survived by anchoring and subsequently maintained the reentrant activity. Thus, as confirmed by the 3-D PS trajectory plots, the rotor dynamics were destabilized transiently by the DC shock, but restabilized after PS repining. In this heart, application of a 30-V DC shock resulted in generation of multiple PSs exhibiting irregular meandering, and the activation pattern was transformed from VT to VF (Online Supplementary Figure 3A), and application of a high-voltage (50 V) DC shock resulted in a prompt disappearance of reentrant activities by shock-induced phase resetting (Online Supplementary Figure 3B).

Figure 3B is the consequence of a 25-V DC shock, which terminated the reentrant activity in the presence of RC. Before the shock, a single clockwise rotor (PS1) anchored to a site close to the RC region (left, a). DC shock at 25 V created 7 new PSs (PSs2 to 8) of either chirality that meandered following complex trajectories (b and c). Then, PS1-PS3, PS4-PS7, and PS5-PS6 disappeared by mutual annihilation. PS8 moved out of the left margin (toward the posterior surface). PS2 survived and drifted along the periphery of the RC region (d and e). The VT terminated by collision of PS2 with the atrioventricular groove approximately 4 seconds after the DC shock application (top). Figure 3B, right, illustrates the trajectory of PSs plotted on space-time axes.

Figure 4 summarizes the data obtained from 18 sustained VTs (in 12 hearts) without RC and 13 sustained VTs (in 9 hearts) with RC exhibiting visible rotors; 38 and 17 DC shocks were applied without and with RC, respectively. In the cases of cardioversion failure, the mode of SW modification was classified into 3 types: no substantial change, repining of rotors (see Figure 3A), and transformation from VT to VF (see Online Supplementary Figure 3A). In the case of cardioversion success, the mode of SW modification was classified into 2 forms; unpinning of rotors followed by collision and extinction (see Figure 3B), and immediate disappearance of rotors by phase resetting (see Online Supplementary Figure 3B). As shown in Figure 4A, for DC shocks without RC (control), the major mode of success was phase resetting at high DC shock intensities (≥ 50 V); transformation from VT to VF often occurred at intermediate intensities (30 to 40 V), and repining was the major mode of failure at relatively low intensities (20 to 30 V). For DC shocks with RC, in contrast, the major mode of success was unpinning with relatively low intensities (15 to 25 V), and the major mode of failure was no change. Figure 4B compares the success rate of DC cardioversion with and without RC. The intensity-response curve with RC was shifted to the left from that without RC (control) by 17.7 V. Average time to VT termination tended to be longer in the presence of RC (1.6 ± 1.9 seconds, $n = 13$) compared with that in the absence of RC (0.6 ± 1.2 seconds, $n = 18$), although the difference remained statistically insignificant (Figure 4C).

Effects of RC on VT/VF induced in 3-D hearts

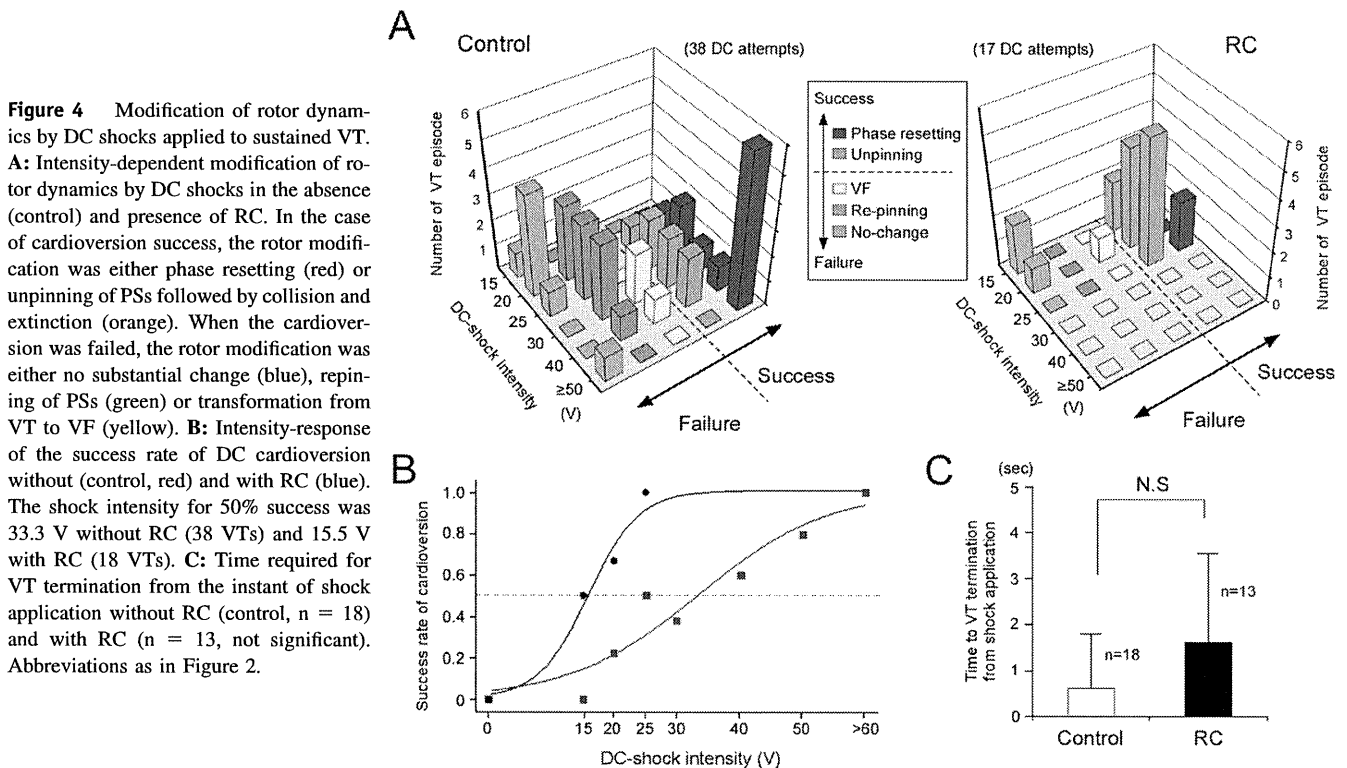
We examined the effects of RC on the sustained VT/VFs (>120 seconds) in 6 intact hearts without cryoablation. A total of 17 sustained VT/VFs were induced. In 8 control VT/VFs, in which RC was not imposed, all (8 of 8) continued during the 30-second observation period. Subsequent application of biphasic DC shocks terminated 3 of 8 VT/VFs. In 9 VT/VFs, in which RC cardioversion was attempted, 1 of 9 terminated within 30 seconds by RC alone; subsequent application of DC shocks in the presence of RC terminated 7 of 8 VT/VFs. The threshold amplitude for the DC cardioversion was 56.7 ± 5.8 V ($n = 3$) in the absence of RC (control), and 31.4 ± 8.5 V ($n = 7$) in the presence of RC ($P < .05$). Time for cardioversion after DC application was 1.3 ± 1.7 seconds ($n = 3$) in the absence of RC and 12.2 ± 11.2 seconds ($n = 7$) in the presence of RC ($P < .05$). DC shocks at the maximum voltage (100 V) failed to terminate 5 of 8 VT/VFs in the absence of RC, but 1 of 8 in the presence of RC. Thus, RC facilitated cardioversion in 3-D hearts when combined with DC shocks in association with a certain modification of the mode of reentry termination.

Discussion

The major findings in the present study are as follows. First, rotors induced during RC were initially confined to the RC region, but were unstable and terminated early by collision following drift. Second, rotors underlying sustained VTs were transformed by RC from stationary to nonstationary; RC terminated approximately 50% of sustained VTs. Third, the threshold intensity of DC shocks for cardioversion of sustained VTs was reduced in the presence of RC; the major mode of rotor termination by DC shocks was changed from phase resetting to unpinning.

RC destabilizes rotors in favor of their termination

In the experiments in which VTs were induced during RC (the first protocol), 98% of the VTs self-terminated within 5 seconds because the rotors were unstable and drifted around the RC region. This finding, which is essentially concordant with a previous report by Boersma et al,¹⁸ can be explained by creation of a region of long refractoriness and reduced conductivity by RC. During constant stimulation, RC prolonged the APD and decreased the CV in the RC region, which explained why the reentrant activity was impaired in the RC region, and was accompanied by intermittent conduction block and long tortuous PS meandering trajectories in the periphery of the RC region. We have previously demonstrated that global myocardial cooling (30°C to 33°C) caused an increase of the maximum APD restitution slope and a broadening of CV restitution curves compared with control subjects.¹⁷ These changes of the restitution properties would increase destabilization of the reentry in the RC region through an enhancement of wavefront-tail interactions.¹⁷ Temperature-dependent alterations of electrotonic effects, short-term memory, and perhaps intracellular Ca^{2+}



dynamics might also contribute to rotor destabilization,⁹ but such factors remain to be elucidated.

Mathematical model analysis of the rotor dynamics has demonstrated that spatial gradients in refractoriness play important roles in the stability of the rotation center in the cardiac muscle with normal excitability.^{21–23} In a medium with stepwise heterogeneity, rotors move along the border separating regions with different refractoriness.²¹ Our observation showing enormous PS drift in the periphery of the RC region is consistent with theoretical prediction.

To assess the potential usefulness of RC for cardioversion, we investigated the effects of RC on sustained VTs and found that RC terminated approximately 50% of sustained VTs. In the cases of successful cardioversion, the rotor dynamics changed dramatically from stationary to nonstationary. The nonstationary rotors shared common features with those induced after RC application in terms of long tortuous FBLs confined to the RC region and tremendous drift of rotors leading to their collision and extinction. The effects of RC on VT perpetuation were reversible upon removal of RC, suggesting a potential advantage of RC as a therapeutic procedure. The failure of RC cardioversion was attributable partly to the topological relationship between the pre-existing rotor and the RC region; when the rotation center was outside the RC region, the success rate of cardioversion was low. The RC cardioversion also depends on the size of the cooling area. In our pilot experiments, we tested the effects of RC to reduce the temperature by approximately 6°C from the baseline (36°C) in a circular area of 3 different size (5, 8, and 10 mm in diameter). Sustained

VTs were terminated efficiently (16 of 33 VTs, 48%) by RC alone only with the largest size tested.

RC reduces the DC shock intensity required for cardioversion

When RC failed to terminate sustained VTs, we attempted DC cardioversion in the presence of RC. Those VTs were likely to be maintained by stationary rotors with PSs anchored at structural discontinuities. Our experiments showed that application of relatively low-intensity DC shocks always created new multiple PSs, resulting from shock-induced virtual electrode polarization.²⁴ SW reentry can be induced by a combination of depolarization and hyperpolarization at a close proximity.^{24,25}

In control subjects (without RC), relatively weak DC shocks caused displacement of preexisting PSs (unpinning) and generated new PSs. Eventually such new PSs disappeared, but organized stationary SW reentry was resumed when the survived PSs were anchored again. Another mode of cardioversion failure was transformation from VT to VF, which was the result of irregular meandering of multiple, widely dispersed PSs. The major mode of cardioversion success in control subjects was immediate PS disappearance by phase resetting at intensities larger than the upper limit of vulnerability.²⁶ In contrast, when DC shocks of weak intensities were applied in the presence of RC, unpinning of PSs was not followed by repinning. Instead, PSs drifted along the periphery of the RC region, eventually colliding and disappearing. Thus, the major mode of cardioversion success in the presence of RC was unpinning. The threshold shock

intensity was reduced significantly (by approximately 50%) from control subjects. Transformation from VT to VF rarely occurred in the presence of RC. These results suggest that RC facilitates DC cardioversion by confining and destabilizing rotors in the RC region.

Ripplinger et al¹⁶ demonstrated in isolated rabbit right ventricular preparations that unpinning and destabilization of rotors leading to VT termination can be induced by weak DC shocks, provided that shocks are applied at a certain phase of the VT cycle.^{16,22} A greater reduction of the DC shock intensity might be possible for cardioversion in combination with RC if the shocks were applied at a restricted phase. Further experimental studies are required to address the issue.

Study limitations

We showed facilitation of VT termination by RC in 2-D ventricular myocardium of rabbit hearts through unpinning and collision of rotors. We used BDM, which is known to affect ion channels and intracellular Ca^{2+} dynamics and to reduce muscle contraction. However, this does not seem to invalidate our results, because characteristic modification of rotor dynamics by RC was preserved in the absence of BDM (Online Supplementary Figure 5). Extrapolation of our observations in 2-D tissue preparations to 3-D and larger hearts is not straightforward. The chance of collision of rotors with boundaries would be reduced, and wave breakup would be enhanced in a larger 3-D tissue mass. In our experiments using intact 3-D rabbit hearts, in fact, RC alone was not effective for self-termination of sustained VT/VFs. However, the threshold intensity of DC shocks for cardioversion was significantly reduced in the presence of RC, and this was associated with an increase in the time required for cardioversion after the shock, suggesting alterations in the mode of reentry termination. Accordingly, a certain benefit of RC favoring low-energy defibrillation is considered to be preserved in 3-D hearts. Structural discontinuities and functional heterogeneities would alter the requirements for rotor termination. In addition, focal activities may also play roles in VT/VF.²⁷ To the best of our knowledge, there are no efficient RC devices applicable to clinical practice, and this is a critical issue to be solved in the future. Despite these limitations, the present study provides a new perspective toward the development of low-energy cardioversion/defibrillation.

Appendix

Supplementary data

Supplementary data associated with this article can be found, in the online version, at doi:10.1016/j.hrthm.2011.08.013.

References

- Buxton AE, Lee KL, Fisher JD, Josephson ME, Prystowsky EN, Hafley G. A randomized study of the prevention of sudden death in patients with coronary artery disease. Multicenter Unsustained Tachycardia Trial Investigators. *N Engl J Med* 1999;341:1882–1890.
- Lee DS, Green LD, Liu PP, et al. Effectiveness of implantable defibrillators for preventing arrhythmic events and death: a meta-analysis. *J Am Coll Cardiol* 2003;41:1573–1582.
- Weaver WD, Cobb LA, Copass MK, Hallstrom AP. Ventricular defibrillation: a comparative trial using 175-J and 320-J shocks. *N Engl J Med* 1982;307:1101–1106.
- Waldecker B, Brugada P, Zehender M, Stevenson W, Wellens HJ. Dysrhythmias after direct-current cardioversion. *Am J Cardiol* 1986;57:120–123.
- Runsiö M, Kallner A, Källner G, Rosenqvist M, Bergfeldt L. Myocardial injury after electrical therapy for cardiac arrhythmias assessed by troponin-T release. *Am J Cardiol* 1997;79:1241–1245.
- Godemann F, Butter C, Lampe F, et al. Panic disorders and agoraphobia: side effects of treatment with an implantable cardioverter/defibrillator. *Clin Cardiol* 2004;27:321–326.
- Kamphuis HC, Verhoeven NW, Leeuw R, Derksen R, Hauer RN, Winnubst JA. ICD: a qualitative study of patient experience the first year after implantation. *J Clin Nurs* 2004;13:1008–1016.
- Jalife J. Ventricular fibrillation: mechanisms of initiation and maintenance. *Annu Rev Physiol* 2000;62:25–50.
- Weiss JN, Qu Z, Chen PS, et al. The dynamics of cardiac fibrillation. *Circulation* 2005;112:1232–1240.
- Biktashev VN, Holden AV. Design principles of a low voltage cardiac defibrillator based on the effect of feedback resonant drift. *J Theor Biol* 1994;169:101–112.
- Morgan SW, Plank G, Biktasheva IV, Biktashev VN. Low energy defibrillation in human cardiac tissue: a simulation study. *Biophys J* 2009;96:1364–1373.
- Garfinkel A, Spano ML, Ditto WL, Weiss JN. Controlling cardiac chaos. *Science* 1992;257:1230–1235.
- Pak HN, Liu YB, Hayashi H, et al. Synchronization of ventricular fibrillation with real-time feedback pacing: implication to low-energy defibrillation. *Am J Physiol Heart Circ Physiol* 2003;285:H2704–H2711.
- Pak HN, Okuyama Y, Oh YS, et al. Improvement of defibrillation efficacy with preshock synchronized pacing. *J Cardiovasc Electrophysiol* 2004;15:581–587.
- Ripplinger CM, Krinsky VI, Nikolski VP, Efimov IR. Mechanisms of unpinning and termination of ventricular tachycardia. *Am J Physiol Heart Circ Physiol* 2006;291:H184–H192.
- Li W, Ripplinger CM, Lou Q, Efimov IR. Multiple monophasic shocks improve electrotherapy of ventricular tachycardia in a rabbit model of chronic infarction. *Heart Rhythm* 2009;6:1020–1027.
- Harada M, Honjo H, Yamazaki M, et al. Moderate hypothermia increases the chance of spiral wave collision in favor of self-termination of ventricular tachycardia/fibrillation. *Am J Physiol Heart Circ Physiol* 2008;294:H1896–H1905.
- Boersma L, Zetelaki Z, Brugada J, Allesie M. Polymorphic reentrant ventricular tachycardia in the isolated rabbit heart studied by high-density mapping. *Circulation* 2002;105:3053–3061.
- Yamazaki M, Honjo H, Nakagawa H, et al. Mechanisms of destabilization and early termination of spiral wave reentry in the ventricle by a class III antiarrhythmic agent, nifekalant. *Am J Physiol Heart Circ Physiol* 2007;292:H539–H548.
- Ishiguro YS, Honjo H, Opthof T, et al. Early termination of spiral wave reentry by combined blockade of Na^+ and L-type Ca^{2+} currents in a perfused two-dimensional epicardial layer of rabbit ventricular myocardium. *Heart Rhythm* 2009;6:684–692.
- Fast VG, Kléber AG. Role of wavefront curvature in propagation of cardiac impulse. *Cardiovasc Res* 1997;33:258–271.
- Fast VG, Rohr S, Gillis AM, Kléber AG. Activation of cardiac tissue by extracellular electrical shocks: formation of 'secondary sources' at intercellular clefts in monolayers of cultured myocytes. *Circ Res* 1998;82:375–385.
- Kléber AG, Rudy Y. Basic mechanisms of cardiac impulse propagation and associated arrhythmias. *Physiol Rev* 2004;84:431–488.
- Efimov IR, Cheng Y, Van Wagoner DR, Mazgalev T, Tchou PJ. Virtual electrode-induced phase singularity: a basic mechanism of defibrillation failure. *Circ Res* 1998;82:918–925.
- Trayanova NA, Gray RA, Bourn DW, Eason JC. Virtual electrode-induced positive and negative graded responses: new insights into fibrillation induction and defibrillation. *J Cardiovasc Electrophysiol* 2003;14:756–763.
- Gray RA, Chattipakorn N. Termination of spiral waves during cardiac fibrillation via shock-induced phase resetting. *Proc Natl Acad Sci USA* 2005;102:4672–4677.
- Tabereraux PB, Dossdall DJ, Ideker RE. Mechanisms of VF maintenance: wandering wavelets, mother rotors, or foci. *Heart Rhythm* 2009;6:405–415.

Images and Case Reports in Arrhythmia and Electrophysiology

Successful Catheter Ablation of Bidirectional Ventricular Premature Contractions Triggering Ventricular Fibrillation in Catecholaminergic Polymorphic Ventricular Tachycardia With *RyR2* Mutation

Takashi Kaneshiro, MD; Yoshihisa Naruse, MD; Akihiko Nogami, MD; Hiroshi Tada, MD; Kentaro Yoshida, MD; Yukio Sekiguchi, MD; Nobuyuki Murakoshi, MD; Yoshiaki Kato, MD; Hitoshi Horigome, MD; Mihoko Kawamura, MD; Minoru Horie, MD; Kazutaka Aonuma, MD

The subject of this report is a 38-year-old woman who often experienced syncope since childhood. Syncope occurred >10 times a year and was associated with convulsion during exercise and emotionally exciting situations. The patient's 13-year-old daughter had also experienced frequent episodes of syncope and developed ventricular fibrillation (VF) during treadmill exercise testing that was successfully defibrillated with electric shock. Witnessing this situation, the patient also lost consciousness, with documented VF that was converted to sinus rhythm by cardiopulmonary resuscitation without electric defibrillation.

Both the patient and her daughter were admitted to our hospital. We performed echocardiography, coronary angiography, and cardiac CT, the results of which revealed no structural heart disease. Resting 12-lead ECG did not indicate any abnormalities, including long-QT syndrome or Brugada syndrome. A signal-averaged ECG revealed no late potentials. Treadmill exercise testing easily induced bigeminal ventricular premature contractions (VPCs) with a right bundle branch block configuration and inferior axis (Figure 1A), and the exercise was terminated because of intolerable symptoms. Catecholamine stress test was started with administration of continuous intravenous infusion of epinephrine in a stepwise manner from 0.025 $\mu\text{g}/\text{kg}$ per minute.¹ During epinephrine infusion at a rate of 0.1 $\mu\text{g}/\text{kg}$ per minute, multifocal VPCs (VPC #1, right bundle branch block configuration and superior axis; VPC #2, right bundle branch block configuration and inferior axis [the same VPC configuration as that induced during the treadmill exercise testing]; and VPC #3, left bundle branch block configuration and inferior axis) appeared, and VPC #1 following VPC #2 subsequently induced VF (Figure 1B).

Administration of bisoprolol 5 mg QD was given but failed to suppress the exercise-induced bigeminal VPCs with the same morphology as induced previously. Because frequent deliveries of shock were believed to be likely, even with β -blocker treatment, catheter ablation was offered to the patient before implantable cardioverter-defibrillator (ICD) implantation. Catheter mapping and ablation for the bidirectional VPCs were performed with a 3D electroanatomic mapping system (CARTO; Biosense Webster) and a 3.5-mm-tip irrigation catheter (NaviStar; Thermo Cool) with only local anesthesia. No VPCs, ventricular tachycardia (VT), or VF were inducible with burst pacing and programmed stimulation from both right ventricular apex and right outflow tract during baseline and continuous intravenous infusion of isoproterenol.

With epinephrine infusion at a rate of 0.1 $\mu\text{g}/\text{kg}$ per minute, VPC #1 and VPC #2 appeared. VPC #1 was nonsustained, and a presystolic Purkinje potential was recorded at the left ventricular inferoseptal area near the posteromedial papillary muscle, which preceded the onset of VPC #1 by 18 ms. The unipolar electrogram from the ablation catheter during VPC #1 showed a QS pattern, and a perfect match of the QRS configuration was obtained by pace mapping (Figure 2). Radiofrequency energy application to this site provoked some ventricular acceleration beats, and several radiofrequency energy applications around the target site finally eliminated all the VPCs, resulting in complete suppression of all VPC #1.

After the ablation of VPC #1, isolated occurrences of VPC #2 continued, and a local bipolar electrogram recorded on the left coronary cusp showed discrete prepotential that preceded the onset of VPC #2 by 65 ms, and a perfect match of the

Received July 26, 2011; accepted January 5, 2012.

From the Cardiovascular Division, Institute of Clinical Medicine (T.K., Y.N., H.T., K.Y., Y.S., N.M., K.A.) and Department of Child Health (Y.K., H.H.), Graduate School of Comprehensive Human Sciences, University of Tsukuba, Tsukuba, Japan; Division of Heart Rhythm Management, Yokohama Rosai Hospital, Yokohama, Japan (A.N.); and Department of Cardiovascular and Respiratory Medicine, Shiga University of Medical Science, Shiga, Japan (M.K., M.H.).

Correspondence to Kazutaka Aonuma, MD, Cardiovascular Division, Institute of Clinical Medicine, Graduate School of Comprehensive Human Sciences, University of Tsukuba, 1-1-1 Tennodai, Tsukuba, Ibaraki 305-8575, Japan. E-mail kaonuma@md.tsukuba.ac.jp

(*Circ Arrhythm Electrophysiol.* 2012;5:e14-e17.)

© 2012 American Heart Association, Inc.

Circ Arrhythm Electrophysiol is available at <http://circep.ahajournals.org>

DOI: 10.1161/CIRCEP.111.966549



Figure 1. A, Twelve-lead ECG recording during treadmill exercise testing. Bigeminal ventricular premature contractions (VPCs) appeared during the second stage of the Bruce protocol. VPC morphology represented a right bundle branch block configuration and inferior axis. Because the patient experienced intolerable symptoms, the test was discontinued. **B**, Epinephrine stress test. Continuous intravenous infusion of epinephrine was started from a rate of 0.025 $\mu\text{g}/\text{kg}$ per minute, and the QT interval did not change. At a rate of 0.1 $\mu\text{g}/\text{kg}$ per minute, VPC #1 (right bundle branch block configuration and superior axis), VPC #2 (right bundle branch block configuration and inferior axis, same as that induced in the treadmill exercise testing), and VPC #3 (left bundle branch block configuration and inferior axis) were induced. Subsequently, VPC #1 following VPC #2 suddenly induced ventricular fibrillation, which was successfully terminated with electric shock.

QRS configuration was obtained by pace mapping (Figure 3). Radiofrequency energy application to the left coronary cusp abolished VPC #2 4 s after the onset of radiofrequency energy application. After successful catheter ablation of bidirectional VPCs, neither VPCs nor VF were inducible, even with an infusion of epinephrine of up to 1.2 $\mu\text{g}/\text{kg}$ per minute (a >10 times higher dose than provocation). Precise ablation sites in a 3D electroanatomic mapping merged with contrast-enhanced CT are shown in Figure 4.

ICD implantation was performed, and the patient was discharged from the hospital on bisoprolol 2.5 mg QD. Serial

Holter ECGs after the ablation showed only 3 to 5 isolated VPCs with a different morphology from the previously observed VPCs, and treadmill exercise testing induced no VPCs at the maximal workload. During 16-month follow-up, neither episodes of syncope nor ICD therapy occurred. Genetic analysis revealed a mutation in the ryanodine receptor gene (*RyR2*), and a diagnosis of catecholaminergic polymorphic VT (CPVT) was confirmed (Figure 5).² The patient's daughter was also given a diagnosis of CPVT with same mutation in *RyR2* and had catheter ablation for the origins of bidirectional VT. Although she refused ICD

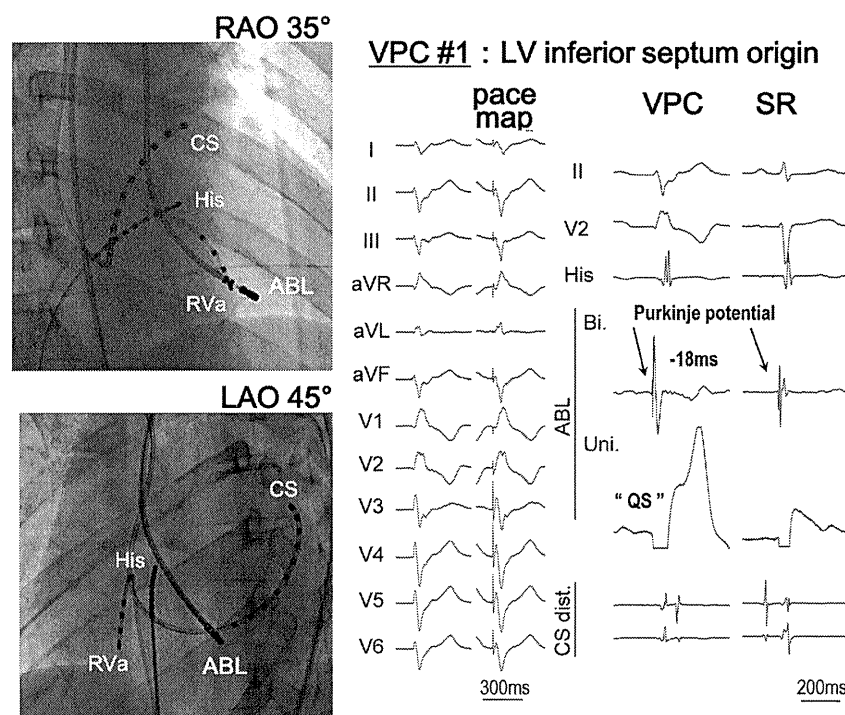


Figure 2. Activation mapping and pace mapping for VPC #1. A Purkinje potential was recorded from the left ventricular inferoseptum and preceded the QRS onset by 18 ms. The unipolar electrogram recorded from the distal electrode showed a QS pattern. Perfect pace mapping was obtained at this site. ABL indicates ablation catheter; CS, coronary sinus; His, His bundle; LAO, left anterior oblique; RAO, right anterior oblique; RVa, right ventricular apex; SR, sinus rhythm; VPC, ventricular premature contraction.

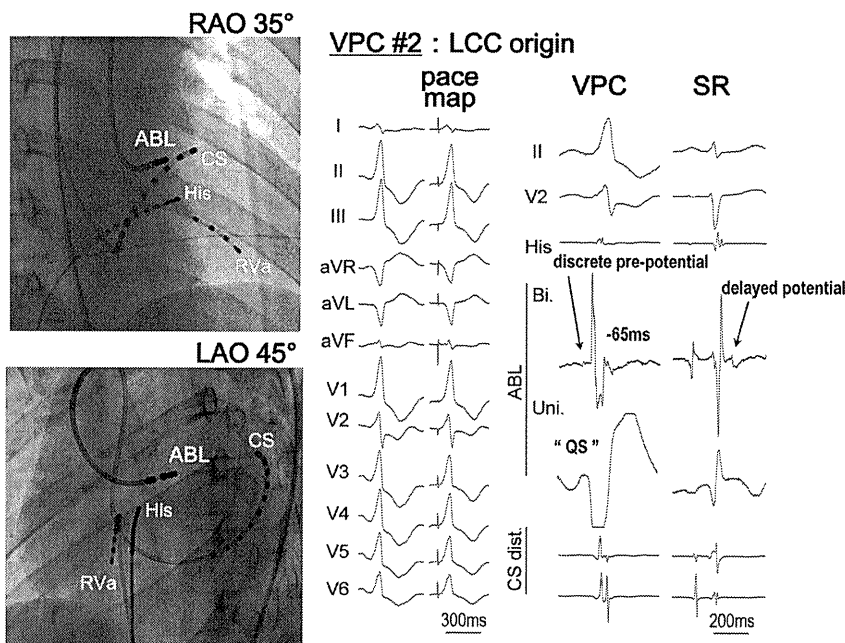


Figure 3. Activation mapping and pace mapping for VPC #2. A local bipolar electrogram recorded from the LCC showed a discrete prepotential that preceded the QRS onset by 65 ms associated with a QS pattern of unipolar electrogram. Perfect pace mapping was obtained at this site. ABL indicates ablation catheter; CS, coronary sinus; His, His bundle; LAO, left anterior oblique; LCC, left coronary cusp; RAO, right anterior oblique; RVa, right ventricular apex; SR, sinus rhythm; VPC, ventricular premature contraction.

implantation, she had not experienced any episode of VT or syncope with β -blocker treatment.

The generally accepted therapy for CPVT has been β -blockers,³ and the additional administration of flecainide or verapamil to β -blockers has been reported to be effective; however, the effects of those drugs are not fully standardized. For medically refractory cases, sympathetic denervation is one of the alternative treatment options. The ICD is considered the definitive therapy for the prevention of sudden cardiac death; however, failure to prevent sudden cardiac death has been reported in several cases because ICD shock delivery might lead to catecholamine release, resulting in an electric storm.⁴ This concern prompted the decision to attempt catheter ablation of VPCs triggering VF. Although

several reports have described successful catheter ablation of VPCs triggering VF in some patients with structurally normal hearts, such as those with Brugada syndrome, long-QT syndrome, and idiopathic VF, successful catheter ablation of VPCs triggering VF in CPVT has not been reported. Cerrone and colleagues⁵ reported that the mechanism of CPVT was due to the delayed afterdepolarization-induced triggered activity in a focal Purkinje network in a knock-in (*RyR2*) mouse. However, whether the Purkinje system is related to the mechanism of VF in CPVT or just trigger origin is still unknown.

To our knowledge, this is the first report of successful catheter ablation of the bidirectional VPCs that trigger VF, and this procedure could become one of the adjunctive

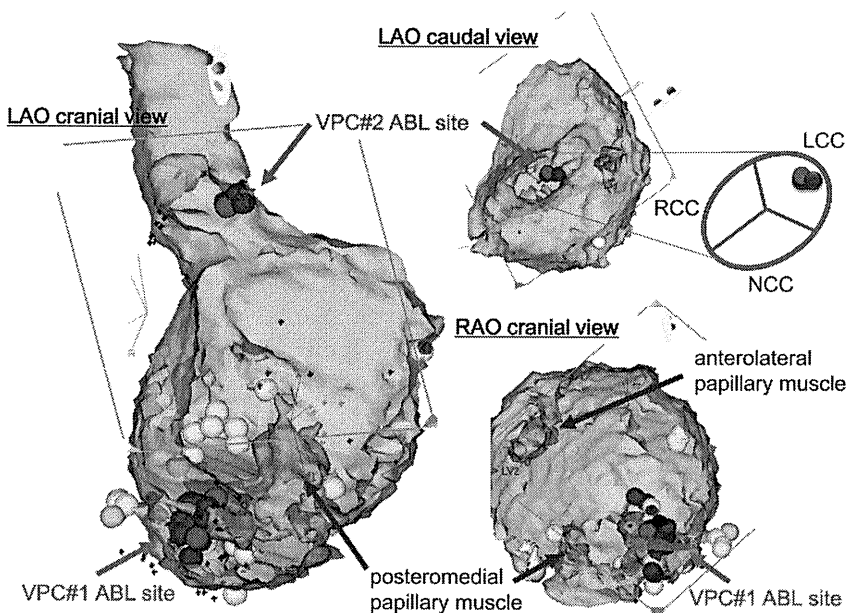
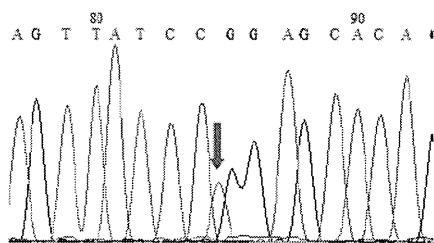
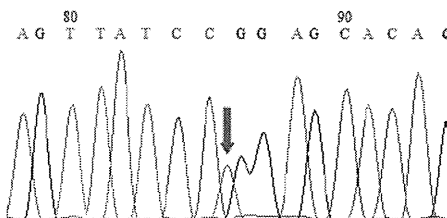


Figure 4. Electroanatomic mapping merged with contrast-enhanced CT. Red tags indicate the ABL sites. Blue tags indicate the sites with perfect pace mapping, and yellow tags indicate the sites with Purkinje potentials during sinus rhythm. The sites with perfect pace mapping and the earliest activation for VPC #1 were localized in the inferoseptal site adjacent to the base of the posteromedial papillary muscle (red arrow). Successful ablation site of VPC #2 was on the left coronary cusp (blue arrow). ABL indicates ablation; LAO, left anterior oblique; LCC, left coronary cusp; NCC, noncoronary cusp; RAO, right anterior oblique; RCC, right coronary cusp; VPC, ventricular premature contraction.

The patient:
RyR2 gene mutation +
1259 G>A (R420Q)



The daughter:
RyR2 gene mutation +
1259 G>A (R420Q)



Sister of the patient:
No mutation

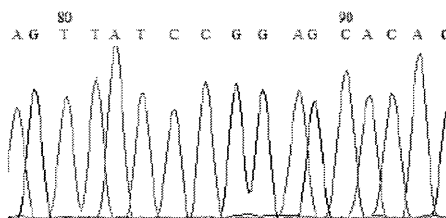


Figure 5. Results of genetic analysis. A mutation in the ryanodine receptor gene (*RyR2*) was detected in both the patient and her daughter. The mutation was not detected in the patient's sister.

therapies in patients with CPVT. To clarify the effectiveness and safety of this procedure, more cases and longer-term observation are mandatory.

Disclosures

None.

References

1. Krahn AD, Gollob M, Yee R, Gula LJ, Skanes AC, Walker BD, Klein GJ. Diagnosis of unexplained cardiac arrest: role of adrenaline and procainamide infusion. *Circulation*. 2005;112:2228–2234.
2. Priori SG, Napolitano C, Tiso N, Memmi M, Vignati G, Bloise R, Sorrentino V, Danieli GA. Mutations in the cardiac ryanodine receptor gene (*hRyR2*) underlie catecholaminergic polymorphic ventricular tachycardia. *Circulation*. 2001;103:196–200.

3. Sumitomo N, Harada K, Nagashima M, Yasuda T, Nakamura Y, Aragaki Y, Saito A, Kurosaki K, Jouo K, Koujiro M, Konishi S, Matsuoka S, Oono T, Hayakawa S, Miura M, Ushinohama H, Shibata T, Niimura I. Catecholaminergic polymorphic ventricular tachycardia: electrocardiographic characteristics and optimal therapeutic strategies to prevent sudden death. *Heart*. 2003;89:66–70.
4. Mohamed U, Gollob MH, Gow RM, Krahn AD. Sudden cardiac death despite an implantable cardioverter-defibrillator in a young female with catecholaminergic ventricular tachycardia. *Heart Rhythm*. 2006;3:1486–1489.
5. Cerrone M, Noujaim SF, Tolkacheva EG, Talkachou A, O'Connell R, Berenfeld O, Anumonwo J, Pandit SV, Vikstrom K, Napolitano C, Priori SG, Jalife J. Arrhythmogenic mechanisms in a mouse model of catecholaminergic polymorphic ventricular tachycardia. *Circ Res*. 2007;101:1039–1048.

KEY WORDS: catecholaminergic polymorphic ventricular tachycardia ■ catheter ablation ■ arrhythmia

Clinical and electrocardiographic characteristics of patients with short QT interval in a large hospital-based population

Akashi Miyamoto, MD, PhD,* Hideki Hayashi, MD, PhD,* Tomohide Yoshino, MD,* Tamiro Kawaguchi, MD,* Atsushi Taniguchi, MD,* Hideki Itoh, MD, PhD,* Yoshihisa Sugimoto, MD, PhD,* Makoto Itoh, MD, PhD,* Takeru Makiyama, MD, PhD,† Joel Q. Xue, PhD,‡ Yoshitaka Murakami, PhD,§ Minoru Horie, MD, PhD*

From the *Department of Cardiovascular and Respiratory Medicine, Shiga University of Medical Science, Otsu, Shiga, Japan, †Department of Cardiovascular Medicine, Kyoto University Graduate School of Medicine, Kyoto, Kyoto, Japan, ‡General Electric Healthcare, Milwaukee, Wisconsin, §Department of Health Science, Shiga University of Medical Science, Otsu, Shiga, Japan.

BACKGROUND Short QT syndrome is one of the underlying disorders associated with ventricular fibrillation. However, the precise prognostic implication of a short QT interval remains unclear.

OBJECTIVE The purpose of this study was to investigate the prevalence and long-term prognosis in patients with a shorter-than-normal QT interval in a large hospital-based population.

METHODS We chose patients with a short Bazett QTc interval from a database consisting of 114,334 patients to determine the clinical characteristics and prognostic value of a short QT interval.

RESULTS A total of 427 patients (mean age 43.4 ± 22.4 years) had a short QT interval with about a 1.2 times higher male predominance (234 men). The QTc interval was significantly longer in female than in male patients (363.8 ± 6.1 ms vs 357.1 ± 5.8 ms, $P < .0001$). The age-specific prevalence of patients with short QT interval was biphasic, peaking at young and old age. Atrial fibrillation and early repolarization were complicated with short QT interval in 39 (9.1%) and 26 (6.1%) patients, respectively. The prognosis of 327 patients (182 men; mean age, 46.4 ± 27.3 years)

with a short QT interval could be assessed (mean follow-up period, 54.0 ± 62.0 months). During the follow-up, 2 patients, 1 of whom had early repolarization, developed life-threatening events, in contrast to 6 patients who died of noncardiac causes and did not have early repolarization.

CONCLUSION The prevalence of a short QT interval showed a slight male preponderance and biphasic age-dependent distribution in both genders. The complication rate of atrial fibrillation was higher in those with a short QT interval than in general populations. The long-term outcome suggested that early repolarization in a short QT interval might be associated with potential risk of lethal arrhythmia.

KEYWORDS Electrocardiography; QT interval; Prevalence; Prognosis; Repolarization

ABBREVIATIONS AF = atrial fibrillation; CI = confidence interval; ECG = electrocardiogram

(Heart Rhythm 2012;9:66–74) © 2012 Heart Rhythm Society. All rights reserved.

Introduction

The QT interval is an invaluable prognostic marker for evaluating whether ventricular arrhythmia occurs.^{1–3} Long QT syndrome is characterized by ventricular cells that fail to repolarize sufficiently quickly. On the other hand, short QT syndrome manifests an extremely abbreviated QT interval.^{4,5} Genetic mutations underlie both syndromes, in which sudden cardiac death occurs.^{6,7} It was reported that short QT syndrome complicated other electrocardiogram (ECG) abnormalities, such as atrial fibrillation (AF)⁴ and early repolarization.⁸ Although close attention must be paid

to short QT interval, there may be overlap between normal QT interval and abnormally short QT interval.⁹ In addition, the prognostic value of short QT syndrome in relation to AF or early repolarization is yet to be determined.

In our university hospital, more than 350,000 ECGs obtained from more than 110,000 patients are available for digital analysis. Using this large hospital-based population, we aimed: (1) to determine the distribution of the QT interval in the entire population, (2) to determine the clinical and ECG characteristics in individuals with short QT interval, and (3) to investigate the prognostic value of short QT interval.

Methods

The research protocol was approved by the Ethical Committee of Shiga University of Medical Science.

Address reprint requests and correspondence: Dr. Hideki Hayashi, Department of Cardiovascular and Respiratory Medicine, Shiga University of Medical Science, Otsu, Shiga 520-2192, Japan. E-mail address: hayashih@belle.shiga-med.ac.jp.

Database

We analyzed resting 12-lead ECGs recorded in the university hospital of Shiga University of Medical Science. The 114,334 consecutive patients (55,091 female and 59,243 male patients) who had undergone ECG recordings between January 1983 and July 2010 were enrolled in the present study. A total number of 359,737 ECG recordings were obtained during this period. The 12-lead ECG was recorded for 10 seconds at a sweep speed of 25 mm/s, calibrated to 1 mV/cm in the standard leads. Twelve leads were simultaneously acquired. The ECG signals were recorded with a temporal sampling interval of 2 ms (i.e., 500 Hz). Digital data were stored in a server computer with 12-bit resolution.

Digital analysis of ECG

MUSE7.1 (GE Marquette Medical Systems, Inc., Milwaukee, Wisconsin) detected an identical P wave and QRS complex with a template matching technique. When AF (defined as irregular RR intervals with fibrillatory waves) was present, only QRS complex was identified by template-matching technique. ECG variables measured were composed by the averaged value during a 10-second recording time. QT interval was measured from the earliest detection of depolarization in any lead (QRS onset) to the latest detection of repolarization in any lead (T wave offset). T wave offset was determined by the time when 98% of the integrated area of T wave was over, which corresponded to a point where the T wave downsloping limb nearly joined the baseline. U wave was excluded. The QTc interval was calculated after correction for heart rate with the Bazett formula. Early repolarization was defined as an elevation at the junction between QRS complex and ST-segment ≥ 0.1 mV from baseline level in at least 2 leads. ST-segment elevation should be present in at least 2 consecutive beats to identify early repolarization. ECG recordings of a mean heart rate < 50 or > 100 beats/min were excluded from the analysis in the first analysis, and then the prevalence of short QT interval in patients with sinus bradycardia < 50 beats/min was additionally investigated. ECGs with ventricular pacing were also excluded. Because all measurements of 12-lead ECG were digitally performed by virtue of software, neither intraobserver nor interobserver variability occurred in this study. To determine whether the automatic measure of QT interval correlates with the manual measure of QT interval, 1,000 ECGs were randomly selected, and then we compared the automatic and manual measure of the QT interval. The manual measure of the QT interval was performed by a standard tangential method in lead V5. The manual QT interval measurement was obtained by averaging the QT interval of 3 consecutive beats.

Data analysis

First, we constructed histograms according to QTc interval. QTc interval divided by 5 ms and the number of ECGs or patients used for frequency density were shown on the abscissa and the ordinate, respectively. Second, the prevalence of patients with a short QTc interval in association

with age and gender was determined. Third, clinical and ECG characteristics of patients with a short QTc interval were determined. The prevalence of AF and early repolarization complicated by short QT interval was determined. Fourth, the prognostic value of a short QTc interval was assessed. Long-term outcome was determined by assessing whether sudden cardiac death, life-threatening ventricular arrhythmia, or any cause of death occurred. Patients were considered to have died suddenly if death was observed and had occurred within 1 hour after new or more serious complaints of probable cardiovascular cause. Life-threatening ventricular arrhythmia was determined by documented ECG. We reviewed the medical records of patients with short QT interval to evaluate their physical health status. In patients whose medical records were not available to determine prognosis, we gathered information on health status by a postal questionnaire. We performed gene analysis (see Supplementary Materials) in patients who developed life-threatening events with short QT interval.

Statistical analysis

The data are presented as mean \pm SD. A comparison between 2 groups was performed with the Student *t* test or the nonparametric Mann-Whitney *U* test, as appropriate. Categorical variables were compared with χ^2 test. Kolmogorov-Smirnov test was performed to determine whether QTc interval distribution fit to a normal distribution. All tests were 2-tailed, and a value of $P < .05$ was considered statistically significant.

Results

In the database, there were 11,416 and 21,450 ECGs with heart rate of < 50 and > 100 beats/min, respectively. We excluded these ECGs from this study, thus 301,345 ECGs derived from 105,824 patients (56.0% men; mean age, 52.6 ± 20.7 years) were included for the analysis of this study. The autonomic QT interval measure was a little but significantly longer than the manual QT interval measure (421.8 ± 23.2 ms vs 418.0 ± 24.5 ms, $P < .0001$).

The mean difference between the manual and automatic QT interval measure was 3.8 ms (median 3.7 ms), and there was a significant linear correlation ($r = 0.95$, $P < .00001$) between the manual and autonomic measure of QT interval (Supplementary Figure 1), indicating the accuracy of the computer-assessed measure of QT interval.

Prevalence of QT interval

Figure 1 shows the distribution of the QTc intervals of total, male, and female patients. The histograms that were constructed as a function of the number of ECGs are shown in the upper row of Figure 1. The mean QTc interval was 421.4 ± 25.7 ms (95% confidence interval [CI] 382 to 482 ms, range 329 to 693 ms) in total patients; 418.9 ± 25.7 ms (95% CI 380 to 480 ms, range 331 to 693 ms) in male patients; and 424.7 ± 25.3 ms (95% CI 387 to 483 ms, range 329 to 687 ms) in female patients. The QTc interval was significantly ($P < .0001$) longer in female patients than

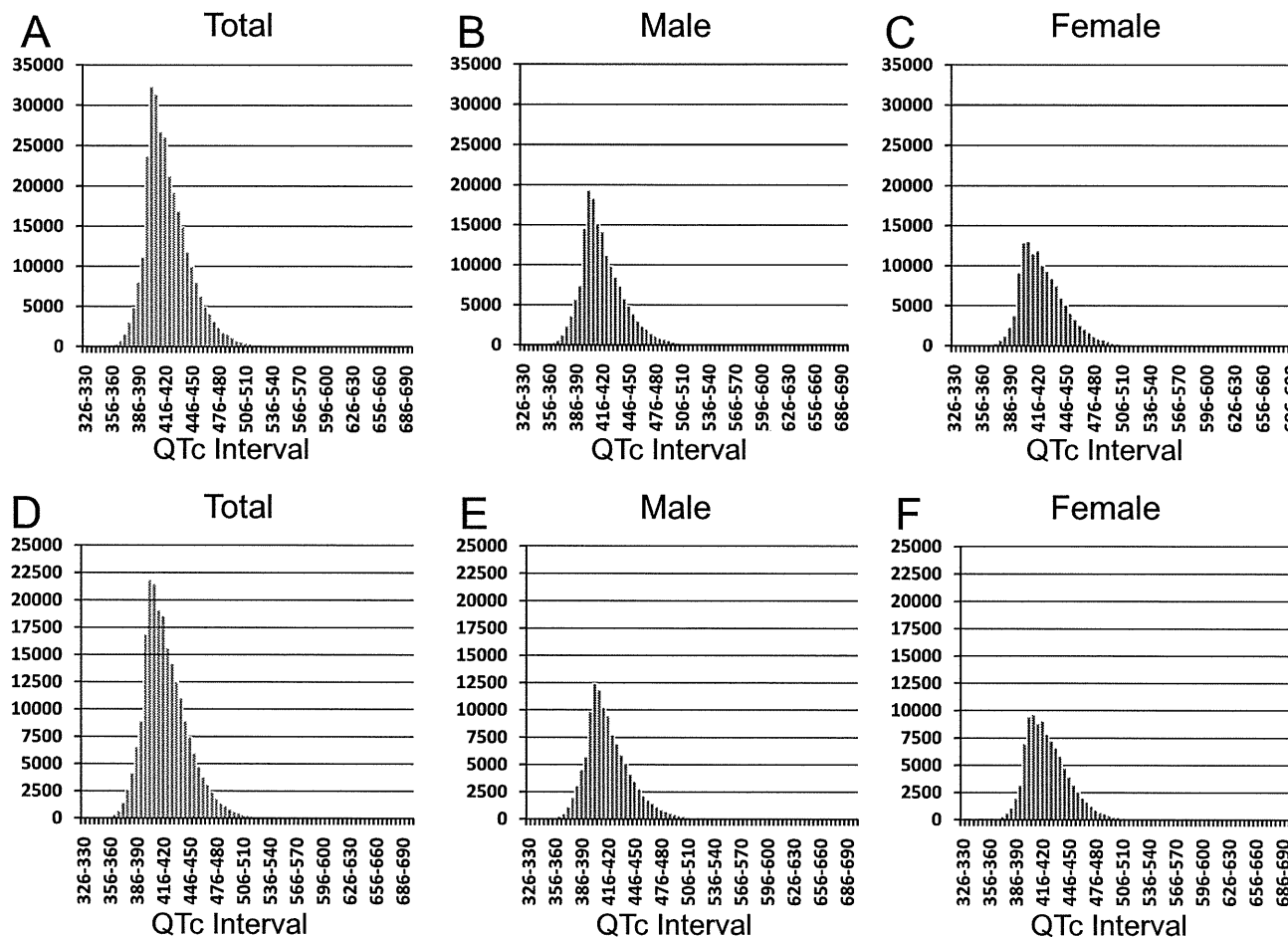


Figure 1 Distribution of Bazett QTc interval according to the number of patients (upper row) and the number of ECGs (lower row). Histograms of total, male, and female patients in this study population are displayed in panels A and D, B and E, and C and F, respectively.

in male patients. The QTc interval distributions did not fit a normal distribution curve ($P < .01$ for each) because the distributions were asymmetrical and right skewed. The histograms of QTc interval that were generated as a function of the number of patients are shown in the lower row of Figure 1. Similarly, the histograms of the QTc interval were right-skewed, which failed to fit to a normal distribution ($P < .01$ for each). The mode of QTc interval was 401 to 405 ms (range 329 to 693 ms), 401 to 405 ms (range 331 to 693 ms), and 406 to 410 ms (range 329 to 687 ms) in total, male, and female patients, respectively. Table 1 shows the lowest percentiles of QTc interval. The QTc interval at the lowest 2.5 percentile was longer than the lower limit of normal QTc interval previously reported.⁹ The QTc interval^{10,11} at the lowest 0.15 percentile was similar to the lower border of QTc interval. We therefore adopted a definition of short QT on the basis of previous studies, the cutoff value matching the 0.15 percentile of our whole population (234 male patients with QTc interval ≤ 362 ms, 193 female patients with QTc interval ≤ 369 ms). Furthermore, we divided the short QT population into percentiles and selected the 2.5 percentile of the short QT population as the very short QT (Table 2).

Clinical characteristics of short QT interval

Four hundred twenty-seven patients with short QT interval were chosen for the analysis according to the abovementioned rationale. The prevalence of patients with a short QT interval was about 1.2 times higher in male patients ($N = 234$) than in female patients ($N = 193$). The mean age was not different between male and female patients (41.9 ± 21.5 years vs 45.2 ± 23.4 years). Table 3 shows clinical characteristics of the patients with short and very short QTc intervals. The mean age was not different between short and

Table 1 The lowest percentiles of Bazett QTc interval for this study population

Percentile	Bazett QTc interval (ms)	
	Male	Female
2.5	380.0	387.0
2.0	378.0	386.0
1.0	373.0	381.0
0.5	369.0	376.0
0.15	362.0	369.0
0.1	361.0	367.0
0.0	331.0	329.0

Table 2 The percentiles for patients with short QT interval

Percentile	Bazett QTc interval (ms)	
	Male	Female
100	362.0	369.0
99.5	362.0	369.0
97.5	362.0	369.0
90	362.0	369.0
75	361.0	368.0
50	359.0	366.0
25	355.0	362.0
10	349.0	355.4
2.5	340.6	345.9
0.5	331.2	329.0
0.0	331.0	329.0

very short QT intervals in both genders. There was a 1.8-fold male predominance in patients with very short QT interval. There are various underlying diseases, in which rate did not differ between short and very short QTc intervals in both genders. Figure 2 shows the age-specific prevalence of total, male, and female patients with short QT interval. The histograms generated according to the number of patients are shown in the upper row of Figure 2. The prevalence was biphasic in each group, with a higher prevalence in young and old adults and with a lower prevalence in middle-aged individuals. The prevalence showed comparable distribution when histograms were generated according to a ratio of patients with short QT interval to total patients in each decade (the lower row in Figure 2).

ECG characteristics of short QT interval

Table 4 lists ECG characteristics. There was no significant difference in various ECG variables between patients with short and very short QT intervals. AF was present in 23 of 234 (9.8%) male and 16 of 193 (8.3%) female patients ($P = NS$). The prevalence of AF did not differ significantly be-

tween patients with short and very short QT intervals in both genders. The prevalence of early repolarization was significantly ($P = .0001$) higher in 23 of 234 (9.8%) male than in 3 of 193 (1.6%) female patients, but was not significantly different between patients with short and very short QT intervals in both genders. In these patients, 11 (42.3%) exhibited early repolarization in anterior leads (V1-4); 9 (34.6%) patients in inferolateral leads (II, III, aVF, V5, 6); and 5 (19.2%) patients in anteroinferior leads (V1-4, II, III, aVF).

Long-term outcome

Long-term prognosis was assessed in 327 of 427 (77%) patients (182 men; mean age, 46.4 ± 22.3 years) with short QT interval. The mean follow-up period was 54.0 ± 62.0 months (range 1.1 to 299.8 months). In patients whose prognosis was evaluated, QT interval was 360.3 ± 24.8 ms and QTc interval was 359.8 ± 7.1 ms. During the follow-up period, 2 male patients developed life-threatening events. One patient was a 22-year-old man who exhibited early repolarization. This patient was admitted to our hospital because he suffered from syncope when drinking in 1989. There was nephritic syndrome in his past medical history, but no family history of cardiac disorders or sudden unexplained death. On admission, 12-lead ECG exhibited early repolarization in ECG leads corresponding to the inferolateral wall of the left ventricle (Figure 3). This patient revealed no evidence of abnormality of cardiac function and morphology by transthoracic echocardiography. Coronary angiography failed to find morphological abnormality, and coronary spasm was not induced by ergonovine injection. However, ventricular fibrillation occurred when the ECG recording was taken after hyperventilation. Because sinus bradycardia preceded the occurrence of ventricular fibrillation, orciprenaline sulfate (30 mg/day) was administered. Seven years later, the patient experienced a storm of ven-

Table 3 Clinical characteristics in patients with short and very short QT intervals

	Male			Female		
	Very short (≤ 355 ms, N = 65)	Short (356 to 362 ms, N = 169)	P value	Very short (≤ 360 ms, N = 36)	Short (361 to 369 ms, N = 157)	P value
Age (yrs)	43.6 ± 23.4	41.2 ± 20.8	.46	46.3 ± 24.9	45.0 ± 23.1	.77
Hypertension (N, %)	13, 20.0	31, 23.9	.54	10, 27.8	27, 26.7	.90
Angina (N, %)	6, 9.2	15, 11.5	.62	1, 2.8	12, 11.9	.08
Myocardial infarction (N, %)	4, 6.2	3, 2.3	.19	2, 5.6	1, 1.0	.14
Valvular disease (N, %)	2, 3.1	8, 6.2	.34	3, 8.3	7, 6.9	.78
Heart failure (N, %)	12, 18.5	22, 16.9	.79	6, 16.7	18, 17.8	.88
Arrhythmia (N, %)	19, 29.2	25, 19.2	.12	7, 19.4	15, 14.9	.53
Diabetes (N, %)	8, 12.3	23, 17.7	.32	4, 11.1	15, 14.9	.57
Dyslipidemia (N, %)	7, 10.8	22, 16.9	.24	6, 16.7	18, 17.8	.88
Follow-up (months)	42.1 ± 47.3	54.0 ± 64.6	.20	49.3 ± 65.7	49.7 ± 62.7	.98
Death (N, %)	3, 4.6	3, 1.8	.24	0, 0	0, 0	—
Ventricular fibrillation (N, %)	1, 4.2	0, 0	—	0, 0	0, 0	—

Arrhythmia involves patients with various types of rhythm disorders, except for patients who exhibited AF when the ECG was taken. Surgery indicates patients who underwent ECG recording before surgical procedure. Others includes patients who suffered various internal diseases or who were suspected to have a cardiovascular disease.

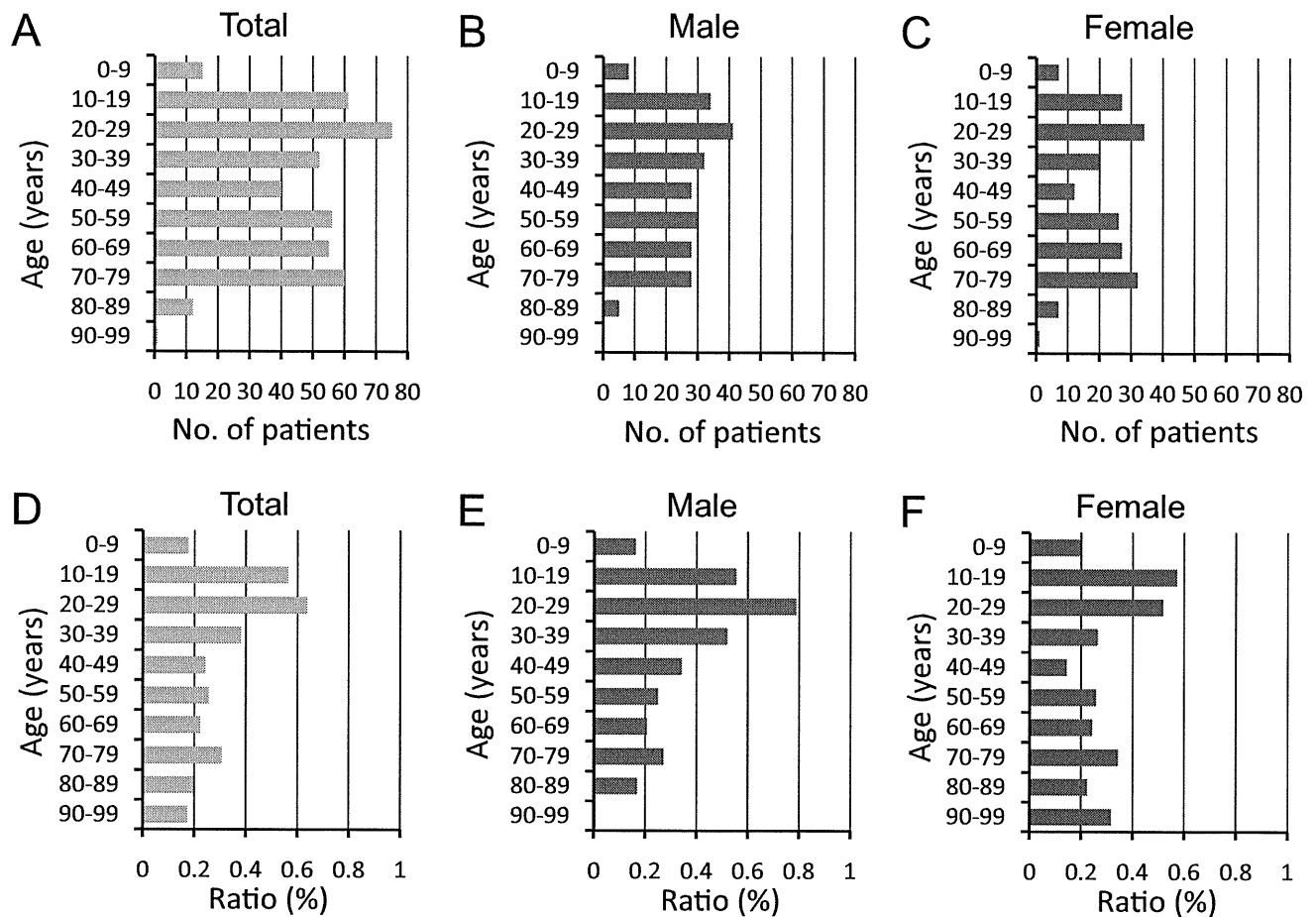


Figure 2 Age-specific prevalence of patients with short QT interval in decades according to the number of patients (upper row) and a ratio of patients to the total population of this study (lower row). Histograms of total, male, and female patients are displayed in panels A and D, B and E, and C and F, respectively.

tricular fibrillation (5 repetitive attacks per day) that occurred when bradycardia occurred (Figure 3B). A ventricular pacing lead was emergently introduced into the right ventricle to maintain rapid heart rate. Subsequently, a permanent pacemaker was implanted (DDDR mode, 80 beats/min). Six years after the storm, ventricular fibrillation recurred during a routine pacemaker check. Ventricular fibrillation repeatedly initiated after bradycardia because of

threshold margin check. The patient received an implantable cardioverter-defibrillator with atrioventricular sequential pacing applied at a rate of 85 beats/min. Another 54-year-old man developed repetitive syncopal episodes with urinary incontinence in 2001 when sleeping. This patient did not exhibit early repolarization (Figure 4). He did not have a family history of cardiac disorders or sudden unexplained death. This patient revealed no evidence of abnor-

Table 4 ECG characteristics in patients with short and very short QT intervals

	Male			Female		
	Very short (≤ 355 ms, N = 65)	Short (356 to 362 ms, N = 169)	P value	Very short (≤ 360 ms, N = 36)	Short (361 to 369 ms, N = 157)	P value
Heart rate (beats/min)	58.7 \pm 8.3	60.3 \pm 8.5	.20	60.6 \pm 8.5	63.3 \pm 9.8	.13
P wave axis (degree)	49.2 \pm 37.5	47.8 \pm 25.3	.77	47.7 \pm 29.4	38.8 \pm 28.5	.12
PQ interval (ms)	165.4 \pm 37.2	163.4 \pm 36.9	.75	161.7 \pm 46.6	156.3 \pm 39.0	.50
QRS complex duration (ms)	92.6 \pm 8.4	92.3 \pm 10.0	.82	87.5 \pm 7.9	85.9 \pm 8.4	.30
R wave axis (degree)	49.3 \pm 32.8	57.3 \pm 27.1	.060	50.6 \pm 31.7	53.4 \pm 26.4	.58
QT interval (ms)	357.4 \pm 23.7	362.6 \pm 22.9	.12	355.4 \pm 25.0	360.2 \pm 25.8	.31
T wave axis (degree)	46.8 \pm 48.5	48.0 \pm 34.9	.83	43.2 \pm 45.4	48.0 \pm 56.7	.64
Atrial fibrillation (N, %)	10, 15.4	13, 7.7	.089	1, 2.8	15, 9.6	.14
Early repolarization (N, %)	3, 4.6	20, 11.8	.076	1, 2.8	2, 1.3	.54

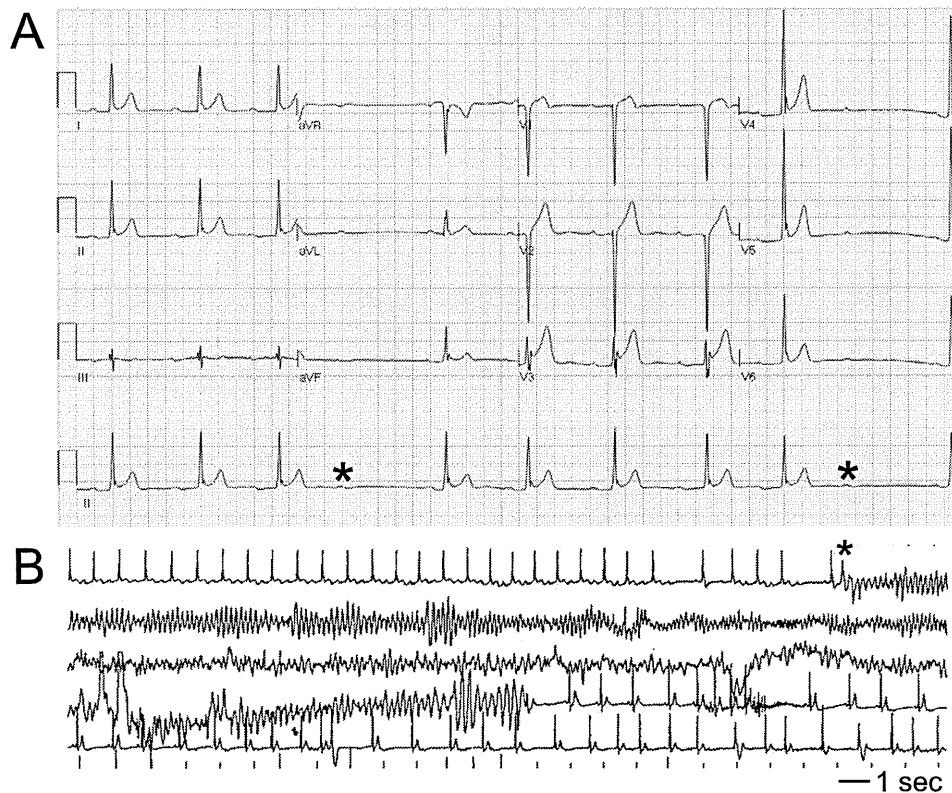


Figure 3 A: Twelve-lead ECG of a 22-year-old male patient who developed ventricular fibrillation. Mean heart rate is 50 beats/min; mean QT interval, 364 ms; and mean QTc interval, 332 ms. Early repolarization is present in leads I, II, aVF, and V3-6. *Nonconducting P wave due to Wenckebach atrioventricular block. B: Monitored ECG showing occurrence of ventricular fibrillation. *A short-coupled ventricular premature contraction initiated ventricular fibrillation that lasted for >1 minute and then self-terminated.

mality of cardiac function and morphology by transthoracic echocardiography and coronary angiography. His ECG showed Brugada-type ECG after intravenous administration of pilsicainide (Figure 4B). The ST-segment elevation in right precordial leads was accepted as sign of Brugada syndrome in the context of a clinical history, suggesting malignant syncope in this patient. To secure this patient from sudden death, an implantable cardioverter-defibrillator was implanted. These 2 patients did not have gene abnormalities, including *KCNQ1*, *KCNH2*, and *SCN5A*. In addition, we confirmed 6 deceased patients: 2 patients died of pneumonia at 70 and 72 years of age; 1 patient, congestive heart failure at 74 years of age; 1 patient, pancreatic cancer at 70 years of age; 1 patient, colon cancer at 74 years of age; and 1 patient, an unknown cause at 79 years of age. These 6 patients did not have early repolarization. AF was present in 1 patient who died of pneumonia.

Discussion

In the present study, we demonstrated detailed characteristics of patients with short^{10–12} QT interval in a large hospital-based population. Consistent with previous reports, patients with short QT interval were rare and had a male preponderance. The age-specific prevalence of patients with short QT interval showed a biphasic distribution with a relatively low prevalence in middle-aged patients. Long-

term prognostic assessment revealed that 2 male patients with short QT interval suffered from life-threatening events in this study population.

Characteristics of short QT interval

The present study disclosed distinct characteristics regarding patients with short QT interval. The gender difference in the prevalence of short QT interval that was manifested in this study is presumably due to sex-specific biology, including hormone, membrane ion channel availability, and intracellular signal transduction. A male predominance of patients with short QT interval shown in this study is similar to the fact that QT interval is generally longer in female^{13–15} than in male patients. Of interest, the pattern of prevalence of patients with short QT interval exhibited inhomogeneous distribution with 2 peaks at young and old ages in both genders. Although we do not know the mechanism by which this age-dependent distribution had 2 peculiar peaks in patients with short QT interval, one can speculate that the underlying mechanism of short QT interval may be different between young and aged patients because health condition is apparently diverse between them. Further investigations will be needed to explore the mechanism underlying the gender difference and age-specific distribution. Contrary to a previous report,¹¹ the prevalence of short QT interval in patients with heart rate of <50 beats/min (male, 2.4%;